A Study in Friction Stir Welding on Marine Grade Dissimilar Metals

Dissertation submitted in partial fulfilment of the requirements for the award of Master of Technology in Marine Technology

By

Harshit C

(Reg. No.: 2201215003)

Under the guidance of

Dr. Sadananda Chakraborty

(Faculty, IMU Kolkata Campus)

Department of Marine Engineering

Indian Maritime University Kolkata Campus

Kolkata 700088

July 2024

INDIAN MARITIME UNIVERSITY KOLKATA CAMPUS

DEPARTMENT OF MARINE ENGINEERING

CERTIFICATE

This is to certify that the dissertation entitled **"A Study in Friction Stir Welding on Marine Grade Dissimilar Materials"** submitted by **Mr. Harshit C** (2201215003) of the Department of Marine Engineering, Indian Maritime University (Kolkata campus), in partial fulfillment of the requirement for the award of the degree of **Master of Technology** in Marine Technology, is a record of bonafide research work carried out under my supervision and guidance.

The content of the dissertation does not form a basis for the award of other degrees to his/her, to the best of my knowledge. The dissertation, in my opinion, is worthy of consideration for the award of the degree **Master of Technology** in Marine Technology following the regulation of the institute

Dr. Sadananda Chakraborty Supervisor Indian Maritime University Kolkata Campus, Kolkata, West Bengal 700088 India	**Dr. Amarish Kumar Shukla** Course Co-ordinator Indian Maritime University Kolkata Campus, Kolkata, West Bengal 700088 India	**External Examiner**

EVALUATION SHEET

Name of candidate	Harshit C
Title of the project	A STUDY IN FRICTION STIR WELDING ON MARINE GRADE DISSIMILAR METALS
Specialisation	Marine Technology
Date of Examination	

The board approved this dissertation for the exam

External Examiner:

Internal Examiner:

COPYRIGHT AND CONSENT FORM

To ensure uniformity of treatment among all contributors, other forms may not be substituted for this form, nor may any wording of the form be changed. This form is intended for original material submitted to the Indian Maritime University, Kolkata Campus (IMU-KC), Kolkata and must accompany any such material to be published by the (IMU-KC). Please read the form carefully and keep a copy for your files.

TITLE OF THESIS:	A STUDY IN FRICTION STIR WELDING ON MARINE GRADE DISSIMILAR METAL
AUTHOR'S NAME and ADDRESS:	HARSHIT C, NO. 32, 7th CROSS, SIR MANJUNATH NAGAR, KALKERE EXT., BENGALURU 560016

COPY RIGHT TRANSFER

The undersigned hereby assigns to Indian Maritime University, Kolkata Campus (IMUKC), Kolkata, all rights under copyright that may exist in and to: (a) the above work, including any revised or expanded derivative works submitted to the (IMU-KC), by the undersigned based on the work and (b) any associated written or multimedia components or other enhancements accompanying the work.

CONSENT AND RELEASE

In the event, the undersigned makes a presentation based upon the work at a conference hosted or sponsored in whole or in part by the (IMU-KC), the undersigned, in consideration for his/her participation in the conference, hereby grants the (IMU-KC), the unlimited, worldwide, irrevocable permission to use, distribute, publish, license, exhibit, record, digitize, broadcast, reproduce and archive; in any format or medium, Whether now known or hereafter developed:

(a) his /her presentation and comments at the conference;

(b) any written materials or multimedia files used in connection with his/her presentation and;

(c) any recorded interview with him/her (collectively, the “Presentation").

The permission granted includes the transcription and reproduction of the Presentation for inclusion in products sold or distributed by (IMU-KC) and a live or recorded broadcast of the Presentation during or after the conference.

In connection with the permission granted in Section 2, the undersigned hereby grants (IMU-KC) the unlimited, worldwide, irrevocable right to use his/her name, picture, likeness, voice and biographical information as part of the advertisement, distribution and sale of products incorporating the Work or Presentation, and releases (IMU-KC) from any claim based on the right of privacy or publicity.

The undersigned hereby warrants that the Work and Presentation (collectively, the "Materials") are original and that he/she is the author of the Materials. To the extent the Materials incorporate test passages, Figures, data or other material from the works of others, the undersigned has obtained any necessary permissions.

GENERAL TERMS

- The undersigned represents that he/she has the power and authority to make and execute this assignment.
- The undersigned agrees to indemnify and hold harmless the (IMU-KC) from any damage or expense that may arise in the event of a breach of any of the warranties set forth above.
- In the event the above work is not accepted and published by the (IMU-KC) or is withdrawn by the author(s) before acceptance by the (IMU-KC), the foregoing copyright transfer shall become null and void and all materials embodying the work submitted to the (IMU-KC) will be destroyed.
- For jointly authored works, all joint authors should sign, or one of the authors should sign as an authorized agent for the others.

Harshit C
(Reg. no.: 2201215003)
Master of Technology
Dept. of Marine Engineering
Indian Maritime University
Kolkata

Contents

ACKNOWLEDGEMENT

I would like to extend my heartfelt gratitude to all those who have supported and guided us throughout this project. First and foremost, I express my sincere appreciation to the Indian Maritime University, Kolkata, for providing us with this valuable opportunity and platform to conduct my research and complete this final project.

My special thanks go to Senior Professor Dr. Sadananda Chakraborty, who served as my project guide. His expert guidance, constructive feedback, and constant motivation were crucial in shaping the direction and success of my project. I am indebted to his patience and knowledge, which have significantly enriched my learning experience.

I am deeply grateful to my distinguished Director, Shri Dr. Rangachari PJ, for his visionary leadership and unwavering support. His encouragement and insights have been instrumental in driving our efforts forward.

I also extend my gratitude to Dr. Amarish Kumar Shukla, our Course Coordinator, for his excellent coordination and support throughout the project. His organizational skills and prompt assistance helped us overcome various challenges and ensured the smooth progression of my work. I am thankful to Arindam from the Indian Institute of Engineering Science and Technology (IIEST) Shibpur for his valuable contributions and technical support, which greatly enhanced the quality of my research.

Additionally, I would like to acknowledge the assistance provided by Kepro Technology Laboratory Pvt. Ltd., a NABL-affiliated metal testing laboratory. Their precise testing and analysis played a critical role in validating my research findings. Lastly, I would like to thank my family, friends, and peers for their continuous support and encouragement throughout this journey. Thank you all for your invaluable contributions. This project would not have been possible without your support and guidance.

DECLARATION

I certify that

1. The work contained in the species is original and has been done by me under the guidance of my superior.
2. The work has not been submitted to any other institute for any degree or diploma.
3. I have followed the guidelines provided by the institute in preparing this dissertation.
4. I have confirmed the norms and guidelines given in the ethical code of conduct of the institute.
5. Whenever I have used materials (data, theoretical analysis, figure and text) from other sources, I have given due credit to them by citing them in the text of the thesis and giving the details in reference.

Harshit C
(Reg. no.: 2201215003)
Master of Technology
Dept. of Marine Engineering
Indian Maritime University
Kolkata

List of Figure

List of Table

List of Equation

List of Abbreviation

°C	Degree Celsius, A Unit of Temperature
BM	Base Metal, The Region That is Neither Thermally nor Mechanically Affected
HAZ	Heat Affected Zone, The Weakest Region of Welding
Hv	Vickers Hardness, A Unit of Hardness
J/g°C	Joules per Gram Degree Celsius, A Unit for Specific Heat Capacity
mm	Millimetre, A Unit of Length
mm/min	Millimetre per Minute, A Unit of Speed
MPa	Mega Pascal, A Unit for Stress
rpm	Revolution per Minute, A Unit of Rotating Speed
SZ	Stirring Zone, A Region were Mixing of Metals Takes
TMAZ	Thermo-Mechanically Affected Zone, A Zone That Experiences Deformation and Temperature Variation
W/m°C	Watt per Meter Degree Celsius, A Unit of Thermal Conductivity

ABSTRACT

Friction Stir Welding is an advanced technique for joining dissimilar materials, mitigating traditional welding issues like solidification cracking and distortion. This study explores friction stir welding for marine-grade Aluminium Alloy 6063-T4 (AL6063-T4) and Magnesium Alloy AZ31B (MG AZ31B), highlighting their lightweight and corrosion-resistant properties suitable for marine environments. Chapter 1 provides a comprehensive background, goals, and benefits of the study. It includes detailed analyses of relevant journal articles and modifications of general articles pertinent to this project. To improve both the weld quality and the efficiency of the friction stir welding process. Chapter 2 goes into detail about Tool geometry which is critically examined to enhance weld quality and friction stir welding efficiency. Steady-state temperature analysis identifies the optimal tool shape using "SolidWorks" for superior mechanical and thermal performance. The tool assembly includes a high-speed steel (HSS) drill bit and an H13 tool steel shoulder. In Chapter 3 a custom vertical milling machine welds two alloy plates, modelled independently in ANSYS for thermal analysis. The study uses SOLID70 elements for three-dimensional thermal analysis, with precise boundary conditions to ensure accurate predictions. A tetrahedral mesh captures high-temperature gradients and stress concentrations, providing insights into deformation, stresses, temperature, and welding properties. In Chapter 4, AL 6063-T4 and MG AZ31B alloys are joined using friction stir welding, with specific surface preparation and butt joint configurations. Mechanical testing includes Vickers microhardness and tensile tests, revealing variations in joint hardness and intricate stress-strain behaviours. Failure analysis identifies TMAZ as the primary failure site, emphasizing its diverse texture structures and fracture initiation. Chapter 5 focuses on optimizing hardness and tensile strength through experimental and Computational Fluid Dynamics (CFD) analysis. ANOVA assesses the impact of rotational and travel speeds on tensile strength, finding rotational speed significantly influences tensile strength. Verification runs confirm the effectiveness of optimized parameters, with minor discrepancies suggesting areas for CFD model improvement. Lastly, friction stirs welding successfully welds 6063 T4 and AZ31B alloys at 430–490°C, enhancing microhardness and joint integrity. While joint tensile strength is lower than base materials, optimization at 1120 rpm and 63 mm/min improves yield strength. Future research should explore microstructural analysis, material innovation, application-specific studies, environmental impact, and standardization, underscoring friction stir welding's potential across various sectors.

Chapter 1

Introduction

1.1. Overview

Friction stir welding has emerged as a cutting-edge welding technology, revolutionizing the conventional landscape of metal joining processes. This method, characterized by its ability to produce high-quality, solid-state welds, has proven particularly promising in the joining of disparate metal materials. The welding of disparate metals presents unique challenges due to differences in thermal properties, melting points, and metallurgical behaviours, making conventional fusion welding techniques less suitable. In this context, friction stir welding stands out as a versatile and innovative approach, offering a solution to the intricate task of seamlessly joining metals with distinct compositions.

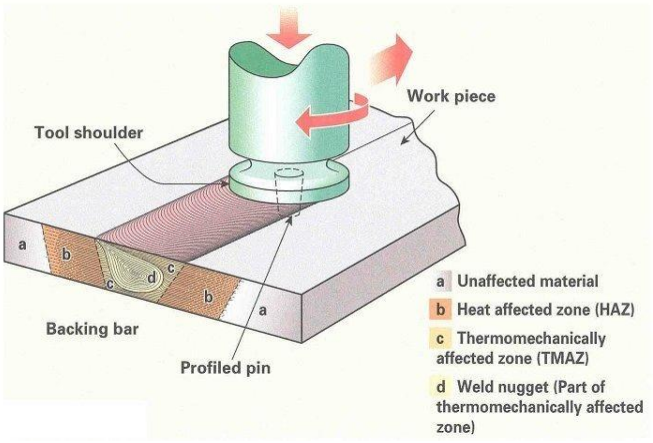

1.1: Friction stir welding (TWI,2019)

The significance of welding dissimilar metal materials extends across several sectors, from manufacturing and aerospace to energy and beyond. These uses require specific supplies with specific properties, often requiring the combination of dissimilar alloys to achieve optimal performance. friction stir welding not only addresses the technical challenges associated with dissimilar metal welding but also opens up fresh opportunities to produce hybrid structures with tailored characteristics.

This exploration focuses on the overarching theme of Friction Stir Welding of Dissimilar Metal Materials, aiming to delve into the fundamental principles, process parameters, and outcomes associated with joining metals that differ in composition, structure, or mechanical properties. By understanding the intricacies of the friction stir welding process applied to dissimilar metals, researchers and engineers can unlock the potential for designing components with enhanced mechanical properties, improved corrosion resistance, and innovative material combinations.

By conducting this study, we hope to add to the growing body of knowledge about friction stir welding and provide guidance for developing new joint configurations, optimizing welding parameters, and establishing standards for strong and dependable dissimilar metal welds. As industries continue to push the boundaries of material performance, friction stir welding of dissimilar metal materials stands as a key technology poised to meet the evolving demands of modern engineering applications.

1.2. Background of Research

In recent years, the joining of lightweight disparate materials has grown more in demand in the manufacturing of hybrid structures and sub-components for various industrial applications. The selection of material combinations for hybrid structures has depended on their strength, density, and metallurgical properties. Lightweight metals, such as aluminium and stainless steel, have exhibited excellent corrosion resistance and high specific strength. According to their exceptional qualities, these materials are crucial for lightweight construction in the chemical and transportation industries, which has helped the equipment reach its goal of versatility [1]. These materials by themselves, meanwhile, haven't been able to sustain the qualities needed for particular applications.

To meet their requirements, the hybrid column structures of aluminium alloy and stainless steel have generated great interest in numerous industrial applications. Conversely, the joining between stainless steel and aluminium alloys has presented difficulties using conventional arc welding techniques because of its formation of brittle intermetallic compounds in the fusion zone [2,3]. To achieve successful joining between these dissimilar metamaterials, solid-state welding methods such as friction stir [4], and friction welding have been contemplated. Other than the joining problems, these processes have several issues with making welds of different joint designs, lengths, and types of joints.

The researchers have studied the joining of these dissimilar metals successfully by using new techniques with tungsten gas welding (TIG)—brazing; this process acts as a welding joint on the aluminium side, and the steel side joint is the same as the brazing joint [5]. The welding process (tungsten-based inert gas fusing-brazing technique) has garnered significant attention lately as a key area of development for the welding of lightweight aluminium alloys and steel. Using an electric stir, this approach melts both substrates and melt consumables, allowing for the junction.

A relatively recent and alluring joining trend, friction stir welding has already attracted a lot of attention in the aerospace industry as an implicit relief trend for engagement. Generally speaking, the procedure is already well-established, especially for blends of aluminium, and the mechanical characteristics of the welds—including the residual stresses—have been repeatedly described. Because it is solid-state, the system can connect various accessories while emulsion-related problems are minimized. However, a great deal of research has been done on welding between various accessories where it may be possible to expect sizable residual stresses. As stated earlier, in conventional fusion welding processes, the liquid filler metal cannot wet and spread as a brazing filler on any surface of the steel. To improve the liquid metal wetting angle of the fillers on substrate surfaces, previous studies have marked that noncorrosive flux can increase the liquid metal wetting angle of fillers in Al brazing, and the molten flux easily adheres to the aluminium hot dip galvanised steel surface [6,7]. However because the solid surface dissolves into the filler metal due to the interaction time between substrates and filler metal, all these processes have helped the production of intermetallic phases. Intermetallic compounds are often more brittle, and when their thickness at the interface goes above the allowable limit, they will restrict the mechanical qualities of the joints.

1.3. Literature Review

According to the current literature, the friction stir welding process parameters—such as tool shape, transverse speed, and rotational speed—have had a substantial impact on the process and have been crucial in determining the weld's quality. It has been claimed that defect-free welds in dissimilar materials from AA5052 to AA2017 were formed when the transverse speed and rotational speed were set at 60 mm/min and 1000 rpm, respectively. Furthermore, the rotating speed or welding speed has increased the tensile strength to a maximum value before it starts to decline as a result of a void defect emerging. Because of the significant softening that takes place in these regions and the irregularly shaped voids that occasionally appear at the advancing side's base metal/weld zone boundary, fracture has been observed in the weld nugget zone at lower welding rates. Moreover, the majority of weld defects have been found at high rotational speeds [8–9].

Friction stir welding with good common edges has been accomplished for several combinations of aluminium amalgamation. In most of these tests, the significant mechanical mixing of the two mixes in the stir zone or weld nugget, with complex whirlpool, spiral, and curve patterns characteristic of chaotic-dynamic mixing. Moreover, it has been shown that the material inflow pattern and subsequent weld quality are significantly influenced by the placement of two different

mixtures. Many investigators have found that it is advantageous to place the more potent of the two accessories on the forward-moving side. The modelling, simulation, and experimental validation of friction stir welding of aluminium alloys using the finite element method were covered in the paper by Nishant A. et al. [10]. Through consideration of tool geometry, rotation, and welding speed, the study seeks to forecast and regulate the temperature distribution during the friction stir welding process. The APDL (ANSYS Parametric Design Language) code from ANSYS commercial software is used in this paper to present detailed thermal modelling of friction stir welding. To determine the temperature distribution inside the welded aluminium plate during the welding process, the authors have also created a transient thermal finite element analysis. The amount of heat transferred into the plate determines the temperature distribution throughout the workpiece, this in turn influences the material flow, microstructure, and mechanical properties of the weld zone. As stated by the paper's conclusion, the temperature gradient through the friction stir welding process can be predicted using the developed model of welding speed, rotation, and tool geometry.

The friction stir welding method of joining dissimilar Almighty 6013-T4 alloy and X5CrNi18-10 stainless steel together was covered in the paper by Huseyin Uzun et al. [11]. The microstructure, hardness, and fatigue characteristics of friction stir-welded 6013 alloys of aluminium to stainless steel were examined by the writers. The study stated that friction stir welding could be used to combine incompatible Al 6013 alloy and stainless steel X5CrNi18-10. The authors characterized the base materials, the heat-affected zone (HAZ), the thermo-mechanical influenced zone (TMAZ), and the weld nugget's microstructure using optical microscopy. The findings indicated that there were seven distinct microstructure zones in the welding: parent stainless steel, weld nugget, TMAZ in the Al alloy at the retreating side of the weld, parent Al alloy, HAZ in the Al alloy at the retreating side of the weld, and HAZ in the stainless steel at the advancing side of the weld. Additionally, the study discovered that the fatigue properties of the Al 6013-T4/X5CrNi18-10 stainless steel joints were roughly 30% less than those of the Al 6013-T6 alloy base metal.

A comprehensive clarification of the application of grinding blend welding innovation for joining distinctive copper to aluminum materials was found by Mehta, K. P., & Badheka, V. J. [12]. The creators examined the grinding mix welding parameters for a divergent Cu–Al framework, such as the tilt point of the instrument, apparatus plan, welding speed, pivoting speed, and workpiece fabric position in the installation. For the Cu-Al grinding mix welding framework, this article moreover talked about the arrangement of intermetallic compounds, microstructure, and welding imperfections. Moreover, the degree of the diverse Cu-Al grinding mix welding system's future

progressions was pondered. The creators did a extraordinary work summarizing the state of the investigate in the subject at that time. The article was well-structured and easy to read. It provided a concise synopsis of the friction stir welding process and demonstrated how to apply it to materials other than copper and aluminum. The writers also did a good job of discussing the challenges of the process and the possible uses of the technology. All things considered, anyone interested in learning more about the friction stir welding approach and its applicability to materials other than copper or aluminum should have checked out this paper.

The effect of process variables on residual stress in stir welds with different friction between age-hardening AA6082 and non-age-hardening AA5083 was covered by Steuwer, A., et al. [13] article. The authors used a systematic set of rotation and traverse speeds to investigate the processing window for the friction stir welding of AA5083 to AA6082. The investigation looked more closely at several microstructurally connected properties, such as precipitate distribution, hardness, and grain size. The predicted and observed thermal distributions were compared and contrasted with the observed variations. To predict the hardness variations across the welds, the thermal model developed in the study was coupled to hardness models based on classical isothermal ageing studies for each alloy. Overall, this paper offered insightful information about how process variables affected residual stress in friction stir welds between age-hardening AA6082 and non-age-hardening AA5083. The authors' summary of the then-current status of the field's research was excellent. The article was easy to read and was organized well. It gave a clear summary of the friction stir welding procedure and how it was used with materials differing from aluminium to copper. The writers also did a good job of discussing the challenges of the process and the possible uses of the technology.

The microstructure, mechanical characteristics, and fracture behaviour of linear friction welded Al-Fe-V-Si alloy 8009 were covered by Baeslack III et al. [14]. A thorough examination of the welded specimens' microstructure, including the growth of the base metal, heat-affected zone, and weld zone, was presented in this work. The writers also discussed the mechanical properties of the welded samples, including their tensile strength, yield strength, and elongation. Additionally, the fracture mode and fracture point of the welded samples were included in the study. According to the study, the Al-Fe-V-Si alloy 8009 could produce high-quality welds through direct disunion welding. The authors recommended further research to better understand how the welding method affected the alloy's mechanical characteristics and microstructure and to improve the welding conditions. All in all, the work offered perceptive information about the microstructure,

mechanical characteristics, and fracture behavior of Al-Fe-V-Si alloy 8009, which had been welded using direct disunion.

An investigation to examine the effects of post-weld treatment on the microstructure and tensile properties of dissimilar friction stir welded AA 2219 and AA 6061 alloys was conducted by Peyre P. et al. [15]. This paper presented a comprehensive analysis of the microstructure of the welded specimens, covering the formation of the base metal, heat-affected zone, and weld zone. The mechanical characteristics of the welded specimens, such as their tensile, yield, and elongation, were also covered by the writers. Additionally, the impact of post-weld heat treatment on the microstructure and mechanical characteristics of the welded specimens was examined. The study concluded that stir-welding AA 6061 and AA 2219 alloys with differing friction significantly improved their mechanical properties through post-weld heat treatment.

Park et al. [16] discovered that when the stronger base material was positioned on the advancing side, the right mixing of material in the nugget region was seen. On the advancing side, there was a discrepancy where a thinner weld nugget and shy mixing passed with weaker material. As seen from the above, depending on the individual pieces of equipment that needed to be joined, successful friction stir welding involved making careful decisions regarding material placement, tool design, and process parameters. An extensive investigation into the impact of the process window (tool gyration and cut speed) on the microstructure, hardness, and morphology of the welds was reported. The study examined a systematic set of AA5083–AA6082 welds and compared them to AA5083–AA5083 and AA6082–AA6082 nascent welds.

Friction stir welding of various alloys between Al blends had been the focus of many experimenters and experts with varying degrees of diligence. When welding similar alloys, it was noted that temperatures were higher on the advancing side. It made sense to think that a more severe temperature asymmetry could result from the arrangement of the alloys in the friction stir welding of various blends. The different mechanical properties and phases, which largely depended on the compositions of the two alloys and the welding parameters like tool rotation speed, travel speed, and positions of the alloys, could be greatly impacted by this asymmetry in temperature, stress, and alloy flow between the advancing and retreating sides. It was noted that the weld interface needed to be on the advancing side to generate sound joints free of defects and that only a small portion of the material migrated from the turbulent flow of the leading-edge experience. More alloy mixing could be achieved when using high-rotation tools at the expense of reduced facial integrity. A thorough analysis of the literature on friction stir welding of copper

and aluminium alloys was provided by Sun, Y., et al. [17]. The writers examined advances and enhancements in the welding process, microstructure, mechanical characteristics, and application relevance of welding technology for copper and aluminium connections as discussed in the paper on the study field of friction stir welding of copper and aluminum. The writers completed their superb assessment of the then-current status of research on the topic. The article was well-structured and easy to read. All in all, anyone interested in learning more about the friction stir welding process and its applicability to materials other than copper and aluminium alloys should have read this paper.

Aval et al. [18] examined the microstructural events and thermo-mechanical behavior when AA5086-O and AA6061-T6 were friction stir welded at different rates. An in-depth examination of the materials' thermo-mechanical behavior during the welding process was provided in this paper, along with a finite element analysis and a three-dimensional model used to predict the materials' thermo-mechanical responses. Additionally, the mechanical characteristics and microstructures in the weld zone were examined. Using model predictions and experimental observations, the authors also investigated the mechanical characteristics and microstructures in the welding area. The authors discovered that when AA5086 was on the advancing side, material mixing in the weld nugget occurred more effectively. Additionally, a greater thermally affected zone was observed on the AA6061 side due to the asymmetric distribution of the temperature field. Microstructural investigations indicated that the fine equiaxed grains forming the stirred zone's microstructures were more prominent on the AA6061 side compared to the AA5086 side. The study suggested that using distinct friction stir welding parameters for AA5086-O and AA6061-T6 could result in high-quality welds.

The authors suggested conducting further research to optimize welding conditions and examine the impact of the welding process on the mechanical properties and microstructure of the alloys. This research provided valuable insights into the thermo-mechanical behavior and microstructural events during dissimilar friction stir welding of AA6061-T6 and AA5086-O. The well-written and organized article made it easier to understand the results and implications of the experiment. It could be challenging for readers who are not familiar with materials science and engineering to grasp the study, however, due to its high level of sophistication. The microstructure and tensile properties of 6061-T6 aluminum alloy after friction stir welding to ultra-low carbon steel were covered by Boumerzoug. et al., [19]. Various advancing speeds of 100, 200, and 400 mm·min−1 at a constant rotation rate were used. The authors used a tensile testing machine to assess joint strength and observed the microstructure using optical and scanning electron microscopy. It was

established that mechanical characteristics and microstructures were interconnected, and that advancing speed affected a joint's shear load. The writers completed their excellent summary of the state of research in the field. The article was well-structured and easy to read. Overall, this study shed important light on the microscopic structure and strength characteristics of ultra-low carbon steel friction stir welded to 6061-T6 aluminium alloy.

Lee et al. [20–21] investigated the joint properties of different formed Al alloys, cast Al alloys, and wrought Al alloys under varying welding conditions as part of another study on the friction stir welding of AA6061 and A356 Al blends. The article provided a thorough analysis of the welded specimens' microstructure, encompassing the development of the base metal, heat-affected zone, and weld zone. The authors also discussed the mechanical properties of the welded specimens, including their tensile strength, yield strength, and elongation. The behavior of the Si particles in cast aluminum alloy and the precipitates of wrought aluminum alloy were connected to the different mechanical properties of the weld zone during the welding process. The microstructure of the welded specimens, including the creation of the weld zone, heat-affected zone, and base metal, was thoroughly examined in their other paper. The creators also examined the mechanical properties of the welded samples, including their ductile strength, yield strength, and elongation. They concluded that by selecting the perfect welding position for the materials and by fine-tuning the welding settings, the combined properties of differently formed aluminum alloys could be improved. Both studies provided valuable data on the microstructure and mechanical characteristics of dissimilar-formed Al alloys. The well-written and organized papers made it simple to understand the results and conclusions of the studies. However, readers who were not familiar with materials science and engineering might have found the articles challenging to grasp due to their high level of sophistication.

Sundaram et al. [22] examined the tensile behavior of stir-welded aluminum alloy joints with dissimilar friction. A thorough analysis of the welded specimens' microstructure, including the growth of the base metal, heat-affected zone, and weld zone, was presented. The authors also discussed the mechanical characteristics of the welded specimens, including yield strength, tensile strength, and elongation. Furthermore, the effect of welding settings on the tensile behavior of the welded joints was investigated. The paper found that the tensile behavior of dissimilar friction stir joined layers of aluminum alloys could be improved by modifying the welding conditions. The authors recommended more research on the impact of welding specifications on the alloy's mechanical characteristics and microstructure. All things considered, the paper offered insightful information about the tensile behavior of stir-welded joints made of aluminum alloys with

dissimilar friction. The well-written and structured paper facilitated comprehension of the experimental findings and conclusions. However, due to its high level of technicality, readers lacking prior experience with mechanical engineering might have found it challenging to understand.

A thorough analysis of the literature on friction stir welding, the processing of different metals with different materials' working tools, and the unique characteristics of titanium alloys was provided by Beygi, R. et al. [23]. The characteristics of plastic flow in friction stir welding and their relationship to adhesion and friction processes were examined by the writers. The friction stir welding of titanium alloys was the primary focus of investigation. The handling of titanium alloys and the selection of working tool materials from various alloys for friction stir welding received particular attention. Additionally, the authors outlined the key advantages and disadvantages of using different tool types for titanium alloy friction stir welding. It was shown how the wear of different tool materials in friction stir welding was linked to the interaction between tools and processed material during welding. Details were provided regarding how this interaction during welding affected the mechanical and functional characteristics of the final joints. Overall, this article offered insightful information about friction stir welding, the processing of different metals using various materials' working tools, and the unique characteristics of titanium alloys. The authors' excellent summary of the state of research in the field was completed. The article was easy to read and well-organized.

The challenges of directly combining dissimilar metals were covered by Rai et al. [24]. This process led to brittle intermetallics at the weld interface, such as FeTi and FexTiy, which weakened the mechanical strength of the joints. An innovative method to prevent brittle intermetallic development was employing interlayers. The paper conducted a comprehensive analysis of several significant friction stir welding tool features, including process economics, geometry and load-bearing capacity, tool deterioration mechanisms, and tool material choices. The authors concluded that the design and material choice of friction stir welding tools had a significant impact on cost, weld quality, and tool performance. Insightful information on optimizing the friction stir welding process design to enhance joint tensile strength during A6005 extrusion was provided in this research. The study highlighted the importance of optimizing friction stir welding process parameters to improve the mechanical properties of joints. In summary, the study provided valuable insights into the friction stir welding process and its applications, emphasizing the importance of using interlayers to enhance joint mechanical strength and prevent brittle intermetallic formation.

A non-consumable rotating tool with a specially designed pin and shoulder was inserted and pushed along the length of the joint after the abutting edges of the layers or plates to be joined were perforated. The tool was primarily used to (a) heat the workpiece and (b) transfer material to form the joint. The piece of equipment was heated through plastic deformation and friction from the tool against the workpiece. The localized heating softened the material around the pin, and the rotation and translation of the tool caused the material to move from in front of the pin to behind it. This process resulted in a solidified joint. Due to the various geometric properties of the tool, the flow of material around the pin could be extremely complex. The extreme plastic deformation of the material at high temperatures during the friction stir welding process resulted in fine and equiaxed reconstituted grains [25–27].

Das, D. et al. [28], presented a numerical analysis of friction stir welding of different materials focusing on tool wear and fault prediction. The authors simulated material mixing and defects (such as surface and subsurface tunnels, exit holes, and flash generation) in friction stir welding of various materials using a coupled Eulerian–Lagrangian technique. Test results on friction stir welding of the candidate pair AA6061 and AZ31B validated the model predictions. To predict weld defects, the impact of tool wear on tool dimensions was experimentally examined for a variety of tool rotation and traverse speed combinations. This data was then integrated into the numerical simulation. The simulation accurately predicted surface tunnels, exit holes, excessive flash formations, and subsurface tunnel defects with a maximum deviation of 1.2 mm. The simulation illustrated the significant influence of plate positioning, whether retreating or advancing, on defect formation; for example, surface tunnel depths reached nearly 50% of the workpiece thickness when AZ31B was positioned on the advancing side. The numerical model effectively represented defect generation resulting from wear-induced changes in tool dimensions. For instance, surface tunnel defects were caused by a 30% reduction in pin length after welding at higher tool rotations and traverse speeds. The study provided a comprehensive explanation of the numerical modeling of friction stir welding of various materials and was well-organized. Along with outlining the study's limitations, the authors suggested avenues for future research.

M. Koilraj et al. [29] has used an optimised friction stirring welding process parameters for dissimilar aluminium alloys AA2219 and AA5083. The study aimed to maximize the tensile strength of the weld joint by optimizing process variables such as tool tilt angle, axial force, traverse speed, and rotational speed. The authors used the Taguchi technique to design experiments, and the analysis of variance (ANOVA) method was employed to evaluate the results. According to the study, the optimal process parameters for friction stir welding of dissimilar

aluminum alloys AA2219 and AA5083 were 1000 rpm for rotation, 50 mm/min for traverse speed, 10 kN for axial force, and 2° for tool tilt angle. The study also found that the tensile strength of the weld joint increased with higher rotational speed and axial force but decreased with increased traverse speed. The study concluded that the Taguchi technique is a useful tool for optimizing friction stir welding process parameters for dissimilar aluminum alloys.

The fine microstructure of friction stir welds contributes to their excellent mechanical properties. The key factors influencing temperature distribution and material flow patterns, which in turn affect the material's microstructural evolution, were tool geometry, welding parameters, and joint designs. Below is a comprehensive list of friction stir welding process parameters:

1. Rotational speed of the tool (rpm)
2. Traverse speed (mm/min)
3. Tool geometry

The friction stir welding tool was central to the process. It heated and softened base materials, extruding them from the top to bottom and from front to rear of the tool, creating solid-state junctions. The shape and material of the tool proved to be the two most critical components of the friction stir welding tool [30]. Throughout the process, the geometry and characteristics of the tool material needed to remain constant. Tool material was shown to be crucial for materials used in workpieces with higher melting points. The success of the friction stir welding process depended on several critical material properties, including room temperature and high-temperature strength, high-temperature stability, wear resistance, tool reactiveness, fracture toughness, machinability, consistency in microstructure and density, and material availability. The most significant benefits of different systems were their simpler tool designs and more affordable tool materials.

Akinlambi et al. [31] investigated the effect of shoulder diameter size on the final weld characteristics of dissimilar friction stir welds between C11000 copper (Cu) and 5754 aluminum alloy (AA). The microstructure of the welded specimens was thoroughly analyzed in this paper, covering the development of the base metal, heat-affected zone, and weld zone. The authors also examined mechanical characteristics such as tensile strength, yield strength, and elongation of the welded specimens. The study examined the impact of shoulder diameter size on the final characteristics of friction stir welds between 5754 aluminum alloy (AA) and C11000 copper (Cu). The study concluded that shoulder diameter size significantly influenced the final weld characteristics of dissimilar friction stir welds between C11000 copper (Cu) and 5754 aluminum alloy (AA). The authors recommended further studies to refine welding parameters and investigate the effects of shoulder diameter size on the microstructure and mechanical properties of other

friction stir welds involving different metals. Overall, the study provided valuable insights into the effects of shoulder diameter size on the final characteristics of dissimilar friction stir welds used to join C11000 copper (Cu) and 5754 aluminum alloy (AA). The well-written and organized article facilitated understanding of the experiment's results and implications.

Zens et al. [32] presented research on friction stir welding of dissimilar metals, focusing on alloys made of copper and aluminum. The study examined how process parameters influenced microstructure and weld quality. The authors also investigated how tool geometry affected weld quality and microstructure. The results demonstrated that friction stir welding of dissimilar metals could produce quality welds with good mechanical properties. The authors discussed challenges and limitations related to friction stir welding of dissimilar metals and made recommendations for further research avenues. The study was well-structured and provided a comprehensive overview of research on friction stir welding of dissimilar metals. The authors' insights will be valuable to researchers and professionals in the field.

Xin Zhao et al . [33] provided an extensive review of the literature on friction stir welding of various materials published over the past 20 years. The authors examined the state of research, welding technology, microstructure, mechanical properties, and process innovations and improvements. Future research areas were suggested, and the report also addressed challenges and limitations associated with friction stir welding of different materials. The study provided a thorough description of research on friction stir welding of dissimilar materials, highlighting any gaps in knowledge. The document was effectively organized and served as a significant resource for scholars and professionals working in the field.

1.4. Summary of Literature Review

The literature addresses the substantial effects that different friction stir welding process parameters have on the quality of welds, particularly when combining dissimilar materials. Tool rotation speed, tool shape, and transverse speed are the critical factors that have been determined to be essential for friction stir welding. The study emphasizes that exact control of these parameters is necessary to achieve defect-free welds, especially between materials like AA5052 and AA2017. Specifically, 60 mm/min longitudinal speed and 1000 rpm rotating speed are recommended. The literature notes that adjusting rotational speed or welding speed can affect tensile strength, with an initial increase followed by a decrease due to the occurrence of void defects. The location of the stronger material, either on the advancing or retreating side, also plays

a critical role in the quality of the weld, with varying outcomes depending on the specific materials being joined and the friction stir welding parameters used.

Furthermore, depending on the characteristics of the materials being joined, the literature highlights the significance of precise material location, device design, and process variables in friction stir welding. Weld quality can be severely impacted by temperature and stress asymmetry caused by the relative positions of the components during the friction stir welding process. The literature also emphasizes how important tool geometry, material, and design are to the friction stir welding process. The literature emphasizes the intricacy of material flow surrounding the friction stir welding tool, which is primarily used for heating and material movement. Good mechanical qualities in friction stir weldings are a result of their fine microstructure. The literature offers a comprehensive list of friction stir welding process parameters, highlighting their influence on the material's microstructural development. These factors include rotating speed, welding speed, and several features of tool shape. Last but not least, the friction stir welding process depends on the selection of the tool's material and geometry, which takes into account factors like machinability, wear resistance, fracture toughness, and strength at both room temperature and high temperature. The significance of choosing the right tool pin shape and dimensions for particular incompatible material combinations is also mentioned in the literature.

1.6 Problem Identification

The journal provides a thorough exploration of recent progressions within the realm of friction stir welding, spanning a diverse array of material combinations [12,14,17,19]. It places particular emphasis on the meticulous investigation of mechanical properties, such as hardness and tensile strength, in conjunction with the examination of microstructural and macrostructural attributes. However, there appears to be a discernible dearth of research dedicated to materials such as Al 6061 and AZ31B, indicating a potential area for future inquiry. [11,13,15,16]

Furthermore, the literature underscores a shortage of studies that establish connections between mechanical and thermal properties and computational fluid dynamics (CFD) simulations, hinting at an opportunity for interdisciplinary investigation. Moreover, the significance of this particular research extends beyond mere experimental analysis. It incorporates the utilization of CFD simulations to scrutinize particle values, thereby expanding the analytical scope [10, 18, 28, 21]. Within this scholarly landscape, a specific study delves into conducting analyses of microstructural and macrostructural characteristics specifically on joints forged via the Friction Stir Welding method, focusing notably on aluminium and magnesium alloy compositions [24,26,27].

Noteworthy is the recognition within some studies of the imperative nature of parameter optimization to augment the mechanical integrity of weld joints. Additionally, it adopts a holistic approach to multi-objective optimization strategies, which contributes substantially to advancing the understanding of friction stir welding processes [29, 31, 32, 33]. This research endeavour not only enriches comprehension but also provides valuable insights for enhancing joint quality through the precise calibration of parameters, the integration of computational modelling techniques and the investigation of mechanical properties.

1.5. The Objective of the Present Research

When conducting friction stir welding of dissimilar metal materials, such as Al6063-T4 to Mg AZ31B, it is significant to define clear objectives to guide the welding process and research efforts. Here's a list of objectives for this specific welding application:

1. Tool Plan: Plan or adjust friction stir welding instruments to oblige the challenges postured by disparate materials like Al6063-T4 and Mg AZ31B, bookkeeping for their varying properties.

2. Computational Demonstrating and Reenactment: Utilize displaying and recreation strategies to anticipate and examine the conduct of disparate fabric friction stir welding, supporting in handle optimization and understanding.
3. Optimal Handle Parameter Choice: Decide the perfect friction stir welding prepare parameters (e.g., rotational speed, navigate speed, device geometry) for joining Al6063-T4 to Mg AZ31B to accomplish high-quality and solid welds.

By laying out these destinations, analysts and engineers can viably arrange and conduct friction stir welding between disparate materials, guaranteeing that the welding handle is optimized for quality, toughness, and unwavering quality in joining Al6063-T4 to Mg AZ31B.

Chapter 2

Material Properties and Tool Design

2.1. Basic Details of Tool and Material

- Friction stir welding Tool

  The two primary parts of the friction stir welding tool are the pin and the shoulder. Important parts of these items include shoulder diameter, shoulder surface angle, pin geometry (size and shape), and the composition of the tool surfaces. In friction stir welding technology, the plasticized material flow, force and torque variations, and heat input are all influenced by the form and design of the tool.

- Tool Shoulder

  The greatest region in friction stir welding that produces heat is the shoulder diameter. It is found that about 87% of the heat is produced by the shoulder due to the rubbing action between the shoulder surface and the workpiece. Tool shoulder diameter and geometry/surface characteristics affect the quality of the weld in friction stir welding because they lead to maximum heat production. The optimal shoulder diameter must be taken into account before welding to create a high-quality friction stir welding joint.

- Tool Pin

  The tool pin's stirring motion is what creates the plasticized material flow in the joint region. The diameter, surface form, and length of the tool pin are all important factors. The pin length determines how much-plasticized material enters the nugget/stir zone. Generally, the tool pin length is kept 0.2 to 0.3 mm shorter than the workpiece thickness to enable the shoulder to provide appropriate axial plunge stress and make correct contact with the workpiece. The pin diameter and surface profile features affect the material flow, microstructure, and stir zone size.

- Al 6063 T4

  AL 6063 T4 is an aluminium alloy that belongs to the 6000 series, which is renowned for its excellent extrudability, corrosion resistance, and weldability. Within this series, AL 6063 is particularly sought after for its favourable combination of mechanical properties and surface finish. The 'T4' designation indicates that the material has undergone a specific heat treatment process to achieve its mechanical properties.

- Mg AZ31B

  Zinc (Zn), aluminium (Al), and magnesium (Mg) make up the composition of the wrought magnesium alloy MG AZ31B. More information is provided in Tables 2.1 and 2.2.

Because of its exceptional mix of qualities—lightweight, good mechanical strength, and corrosion resistance—it is one of the most widely used magnesium alloys.

2.1.1. Chemical Composition and Mechanical Properties

2.1: Chemical composition of materials

Element	Si	Mg	Cu	Fe	Zn	Cr	Al	Mn	others
Wt% of Al6063-T4	0.25	0.45	0.24	0.35	0.1	0.1	Bal.	0.1	0.4max
Wt% of Mg AZ31B	0.1	Bal.	0.5	0.005	1	-	3.2	0.5	0.3max
Wt% of H13 tool steel	0.88	0.35	0.02	Bal.	-	5.04	-	0.35	0.5max

2.2: Mechanical properties of selected material

Properties	Al 6063-T4	Mg AZ31B	H13 Tool Steel
Density	2.69 g/cm^3	1.77 g/cm^3	7.80 g/cm^3
Tensile strength	150Mpa	260Mpa	1400Mpa
Poisson's ratio	0.27	0.29	0.3
Thermal expansion coefficient	23.4 µm/m°C	26 µm/m°C	104 µm/m°C
Thermal conductivity	90W/mk	96 W/mK	28.6 W/mK

2.2. Fabrication of Tool

Apart from fusion-type welding, friction stir welding develops heat through the process of joining the metals themselves. So, a detailed study of tool geometry based on steady-state temperature has revealed a good tool geometry. The modelling is made by the modelling software "Solidworks" for tool geometries. As the tool consists of two parts, the Tool Sholder is fabricated with material H13 tool steel in Lathe with mechanical properties as listed in Table 2.2 and the tool pin is replaced by a high-speed steel (HSS) standard drill bit. Figures 2.1, 2.3, 2.5 and 2.7 show the tool design that is built into the software Solidworks 2019, correspondingly Figures 2.2, 2.4, 2.6 and 2.8 show the fabricated different parts of friction stir welding.

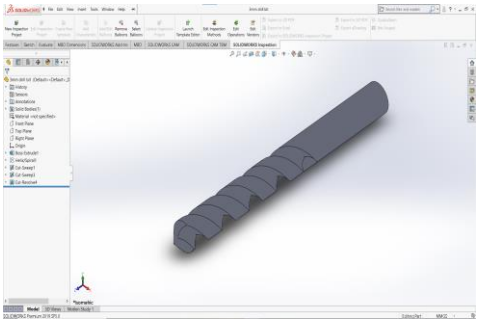

2.1: Tool pin - HSS drill bit in Solidworks

2.2: Fabricated tool pin – HSS drill bit

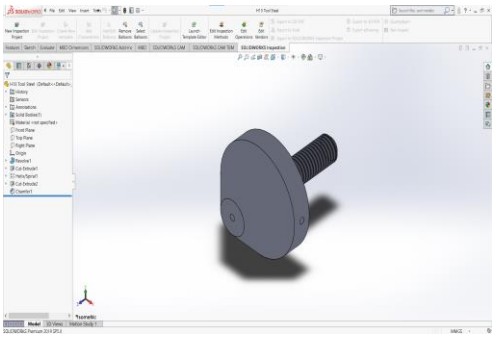

2.3: Tool sholder in Solidworks

2.4: Fabricated tool sholder

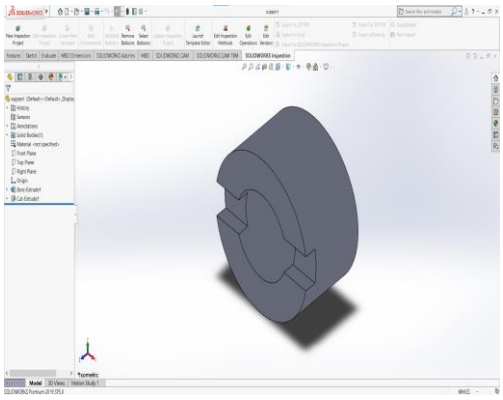

2.5: Tool shoulder support in Solidworks

2.6: Fabricated tool shoulder support

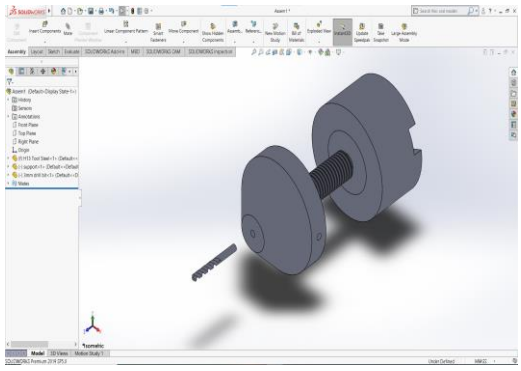

2.7: Exploded view and assembled friction stir welding tool in Solidworks

2.8: Exploded view and assembled fabricated parts

Chapter 3

Computational Fluid Domain

CFD is a branch of studies in liquid mechanics that uses computational tools and mathematical modelling in the study and clarification of concerns like liquid streams. Thus, CFD provides engineers and researchers with the use of numerical models and reenactment to predict the behaviour of the liquid in the specified applications ranging from streamlined features and climate determination to mechanical designs and biomedical structures. It takes a major role in enhancing regular plans, increasing the efficiency of the execution and decreasing the need of physical models which in turn saves time and money while at the same time giving detailed information about the liquids in use.

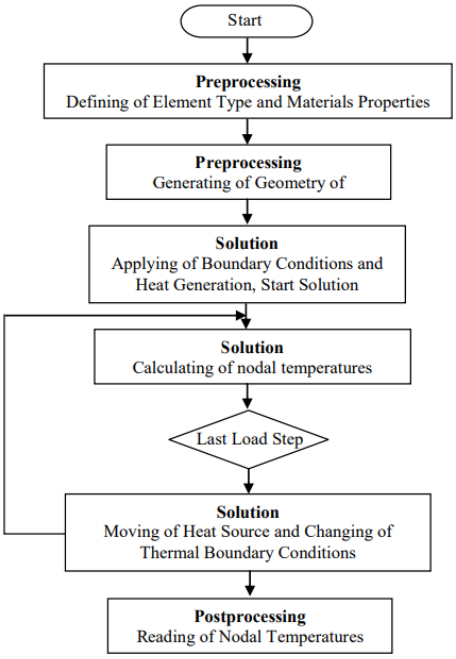

3.1: Block diagram of the procedure followed in CFD

3.1. Modelling

In the vertical milling machine designed for friction stir welding, two alloy plates, Al 6063-T4 and Mg AZ31B, each measuring 100 × 200 × 3.1 mm^3, are lap welded together. The ANSYS program models two plates because of the asymmetry. ANSYS software is utilized to mesh the workpiece in the current thermal study using a brick element known as SOLID70. This element can be applied to three-dimensional, steady-state, or transient thermal analysis due to its three-dimensional thermal conduction capacity. The orthotropic material qualities and the eight nodes, each of which has a temperature as a single degree of freedom, define the element. Using this element has the benefit that it may be swapped out for a structural element that is equivalent to

the structural analysis. The workpiece's finite element model, produced by ANSYS software, is displayed in Figure 3.1. Coupled Field Transits are utilized in ANSYS's finite element studies to provide a subroutine for a transitory moving the source of heat model. Moving heat sources are taken into consideration when doing transient finite element analyses.

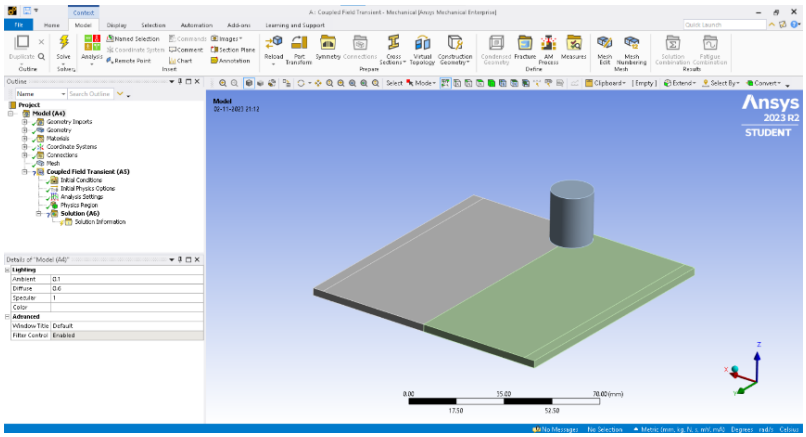

3.2: Model of friction stir welding in ANSYS

3.2. Boundary Condition

It is noteworthy to emphasize that the CFD model's boundary conditions have a big impact on how the outcomes are predicted. It needs to depict the actual physical circumstances of the welding procedure. The definition of the flow inlet boundary condition is:

$$u = u_{inlet}, v = 0, w = 0 \tag{3.1}$$

where u (inlet) is the welding traverse speed and v, w, and u are the magnitudes of the velocities in the x, y, and z directions, respectively. A free slip wall has been defined by the workpieces on the domain's upper, lower, and side surfaces. For the output border, a pressure outlet with a zero pressure value was assumed. In this study, the tool angular translations in the x and z directions (u and w) that are displayed in Eqs. 3.2 and 3.3 is used to specify the velocity components on the tool surface.

$$u = (1 - \partial)(\omega r \sin\theta - u_{weld}) \tag{3.2}$$

$$w = (1 - \partial)(\omega r \cos\theta) \tag{3.3}$$

where ω is the tool speed rotation, represents the angle from the direction of the tool movement with the x-axis, and the value of r between the range of $r_{pin} < r < r_{shoulder}$.

3.3. Meshing

Because mid-side nodes are avoided and often correspond to quadratic interpolation functions for a more accurate representation of the solution, a linear mesh with omitted mid-side nodes is utilized. This is because using mid-side nodes in thermal simulations may cause the temperature distribution to oscillate. These oscillations are undesirable and can result in nonphysical or

unrealistic temperature profiles. To avoid this mesh-orientation dependency, a tetrahedral mesh (which could use triangular or quadrilateral elements in 2D, or tetrahedral or hexahedral elements in 3D) is chosen over a linear mesh. This option contributes to making the simulation results more mesh-orientation-sensitive. A finer mesh is employed in the weld-line region for more accurate results. Welds often experience high-temperature gradients and stress concentrations, and using a finer mesh in this area helps capture more details of the thermal behaviour, providing a more accurate representation of the solution.

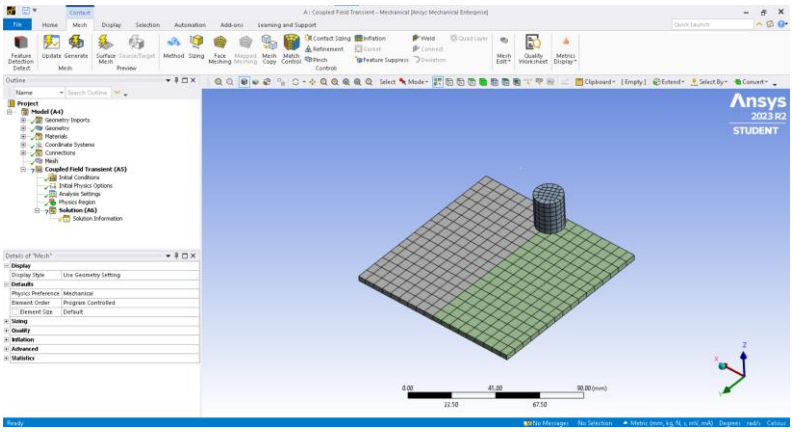

3.3: Meshing in ANSYS

Thermal conductivity, k and heat capacity, Cp are dependent on temperature. Table 3.1 presents the variation of material properties of Al6063-T4 and Mg AZ31B concerning temperature used in the finite element analyses. Additionally, the following W/V ratios (all in units of r/mm) were chosen for the weld pitch, or ratio, between the revolution speed (W) and the speed of travel (V): 1400/31, 1120/25, and 900/16. The boundary condition was given to the walls of the workpiece, where displacement was kept zero in the z-direction and heat convention at the initial was given to a micron.

3.1: Variation of material properties of 6063-T4 and AZ31B concerning temperature.

T (˚ C)	Al 6063-T4		Mg AZ31B	
	K (W/m˚ C)	Cp (J/g˚C)	K (W/m˚ C)	Cp (J/g˚ C)
30	190	0.9	90	0.96
50	193	0.94	93	1
150	195	0.96	95	1.02
200	198	0.99	98	1.05
250	203	1.025	103	1.085
300	207	1.055	107	1.115
350	209	1.08	109	1.14
400	214	1.1	114	1.16
450	216	1.115	116	1.175
500	221	1.125	121	1.185

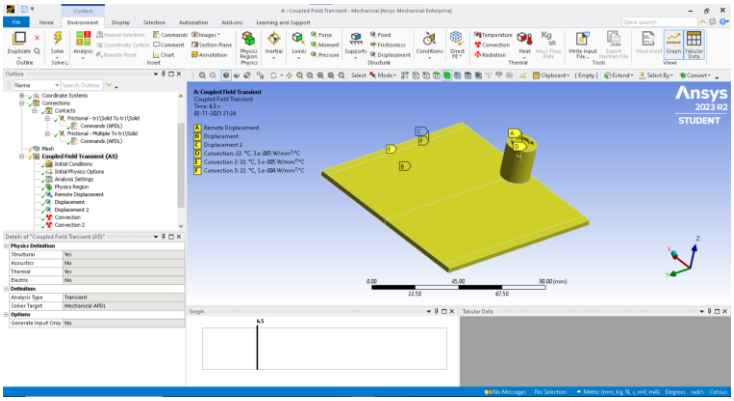

3.4: Model of friction stir welding in ANSYS after boundary condition

3.4. Results and Discussion

The results for friction stir welding are as follows:

1. Deformation and stresses
2. Temperature results
3. Welding results
4. Heat generation
5. Summary of Result

3.4.1. Deformation and Stresses

Throughout the friction stir welding preparation, it is crucial to monitor the changes in various amounts surrounding the weld line. As seen in Figure 3.5, the avoidance results in towering tensions being created on the workpiece underneath the equipment.

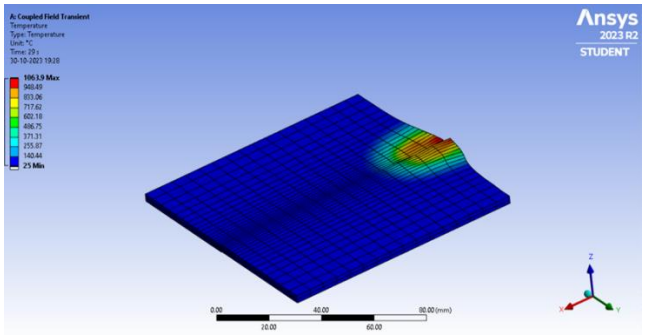

3.5: Von mises stress after load step 1

As shown in Figure 3.6, the temperature stays constant at 25°C after stack step 1:

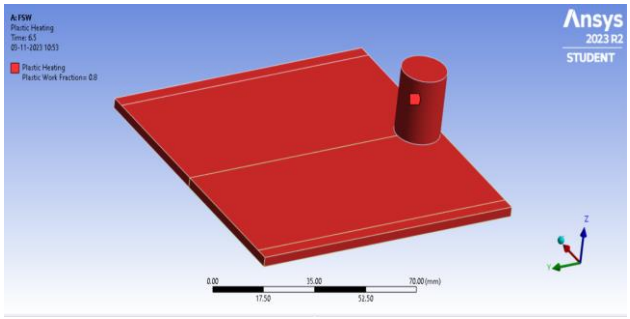

3.6: Temperature after load step 1

Here is where the apparatus begins to turn, creating and increasing frictional stresses rapidly. The following Figures 3.7, 3.8, and 3.9 show the rise in contact frictional stresses between steps 1 and 2 of the stack.

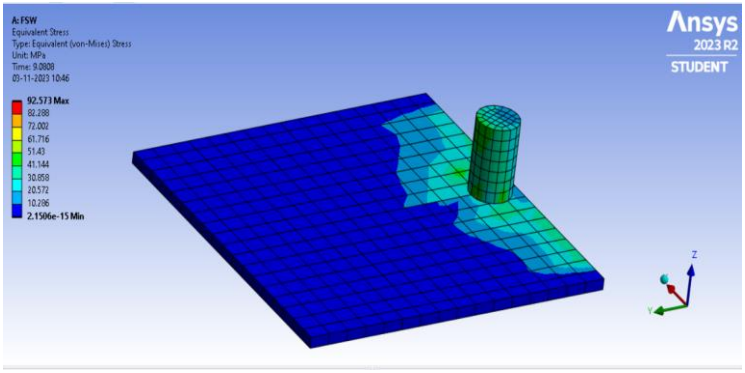

3.7: Von mises stress after load step 1 for speed 900 rpm

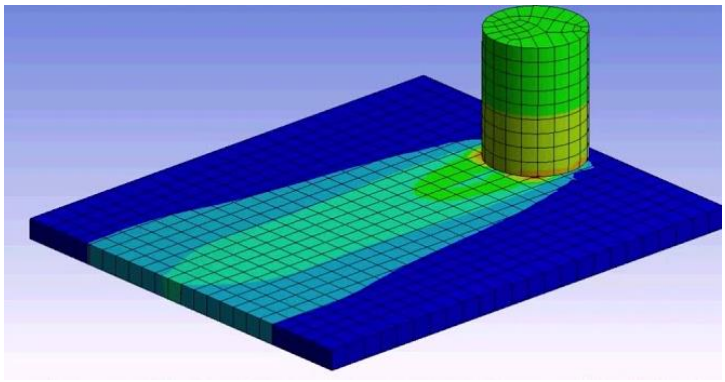

3.8: Von mises stress after load step 1 for speed 1120 rpm

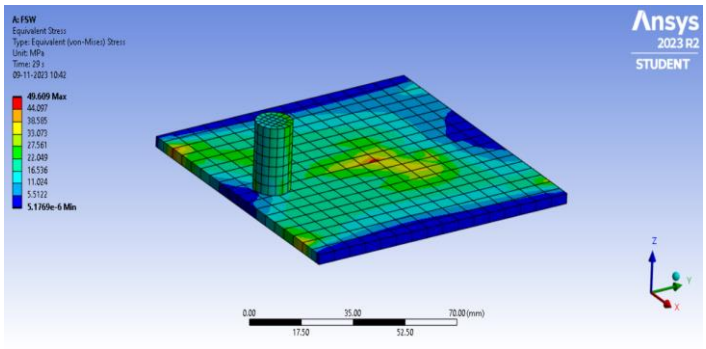

3.9: Von mises stress after load step 1 for speed 1400 rpm

During stack step 2, any frictional energy that is wasted is converted to warm energy. At the tool-workpiece interaction, the warm is generated. The workpiece receives the majority of the warm exchange (FWGT is 0.95).

3.4.2. Temperature Result

Figures 3.10 and 3.11 below illustrate the temperature increase brought on by heat generation in both the second and third load steps:

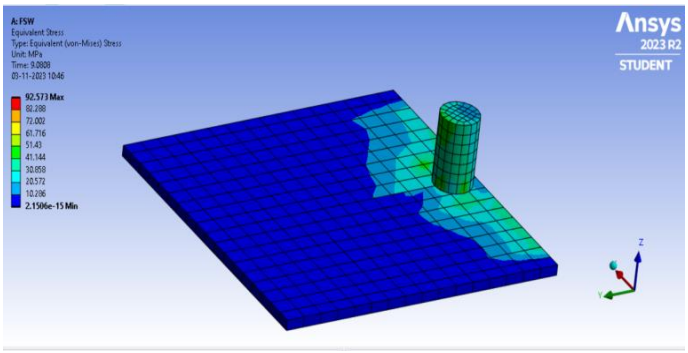

3.10: Temperature after load step 2

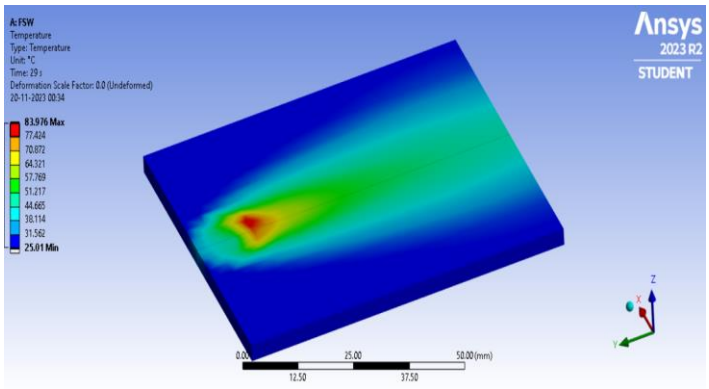

3.11: Temperature after load step 3

The final two load phases are when the workpiece reaches its maximum temperature beneath the tool. The mechanical loads are the cause of heat creation. There is no usage of outside heat sources. The coefficient of friction lowers as the material softens as the temperature rises. The maximum temperature is kept from rising above the material's melting point with a heat-dependent coefficient of friction (0.4 to 0.2). The observed temperature rise in the model demonstrates that plastic deformation of the workpiece material and friction between the tool shoulder and workpiece are the sources of heat generation throughout the second and third load phases. Both the aluminium 6063-T4 and the magnesium AZ31B have a melting point of 600°C. Figure 3.12 illustrates that during the second and third load steps, the highest possible temperature range at the line of welding region on the piece of workpiece beneath the tool is significantly lower than the initial melting point of the workpiece material, but it is still higher than 70% of the melting temperature.

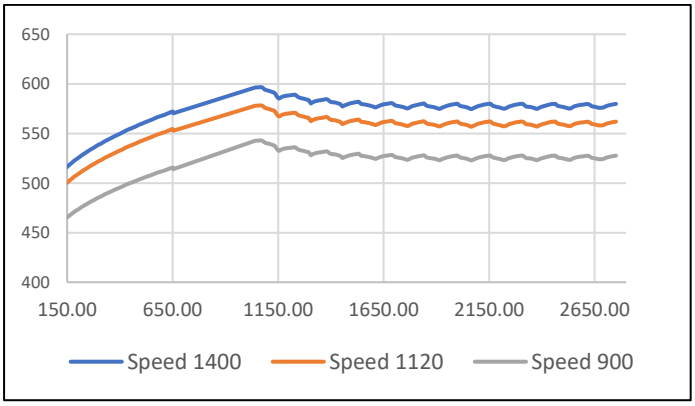

3.12: Maximum temperature variation with respected to time

3.4.4. Heat Generation at Welded Region

Heat is produced by plastic deformation and friction. The creation of plastic and frictional heat is calculated. In the second load step, frictional heat generation starts. Determining the total frictional heat generation rate at every time step is feasible. A bonding temperature of about 500 °C has already been established at the plate interface for the welding simulation. Overall frictional heat generation rate against time is displayed in Figure 3.13 below.

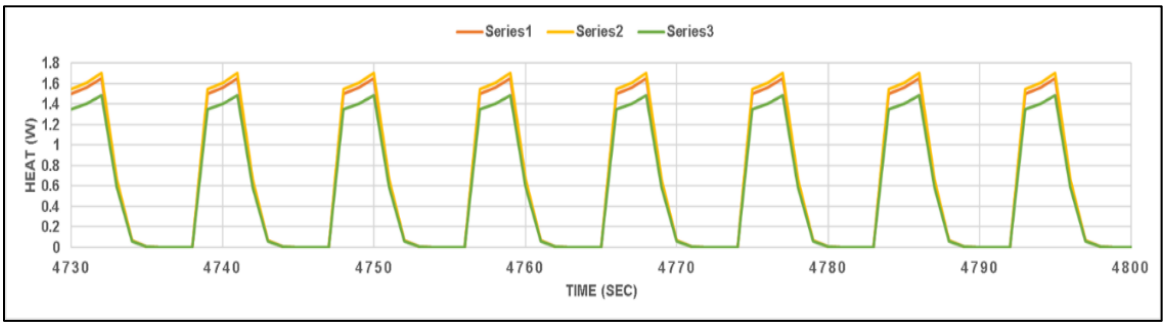

3.13: Heat generation graph of speeds 900,1120,1400 rpm

3.5. Summary of CFD Result

The table provided is a Summary of CFD Results.

3.2: Summary of CFD result

Rotation speed (rpm)	**900**			**1120**			**1400**		
Travel Speed (mm/min)	25	40	63	25	40	63	25	40	63
Stress (Mpa)	153.78	154.46	156.26	166.67	167.34	167.86	162.20	163.28	163.78
Temperature (degree C)	431.9	434.79	439.79	458.57	460.45	461.88	488.79	491.65	493.14

Chapter 4

Experimentation

4.1. Experimental Setup and Methodology

Friction stir welding was used to join Al 6063-T4 alloy and AZ31B magnesium alloy, which had thicknesses of 3.1 and 2.8 mm, respectively. Table 2.1 lists the chemical compositions of both materials. Before welding, the surfaces of both plates were cleaned using acetone and a stainless-steel brush. As seen in Figures 4.1 and 4.2, all welds were completed in the side-ways lap joint configurations of Al 6063-T4 and AZ31B.

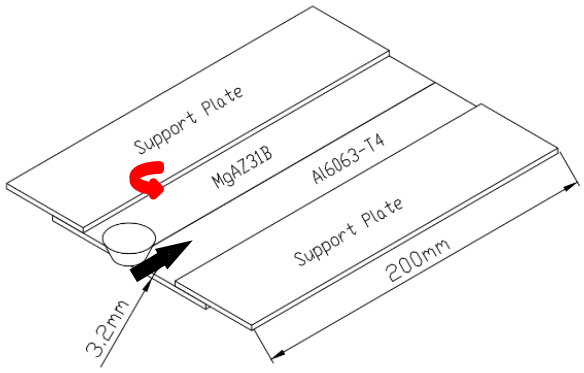

4.1:Isometric view of the setup

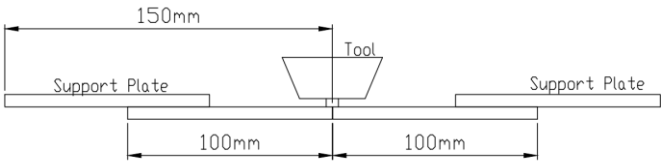

4.2: Front view of the setup

To establish metallurgical binding in a cleft joint disorder, the tool pin's length had to be less than the plate's thickness. The friction stir welding joints were fabricated using an HMT knee HMT-type milling machine FN2/FN3 (7.5/5l5 kW Motor for heavy stock removal, as shown in Figure 4.3) in a displacement-controlled configuration. The tool was angled three degrees forward and rotated clockwise. Because the extra compression of the tool shoulder produced higher heat, tapered pin and slanted conditions were used in this study. Any cavities or tunnels created by the original gap between the welded plates can be eliminated by the additional compression the tilting of the tool causes on the trailing side. The following W/V ratios were used to choose the weld pitch, or ratio, between the rotation speed (W) and travel speed (V). Constant weld pitch ratio

W/V selection has also been used in the past for the friction stir welding of AZ31 to Al 6061 alloys.

4.3: HMT Knee HMT-type milling machine FN2/FN3

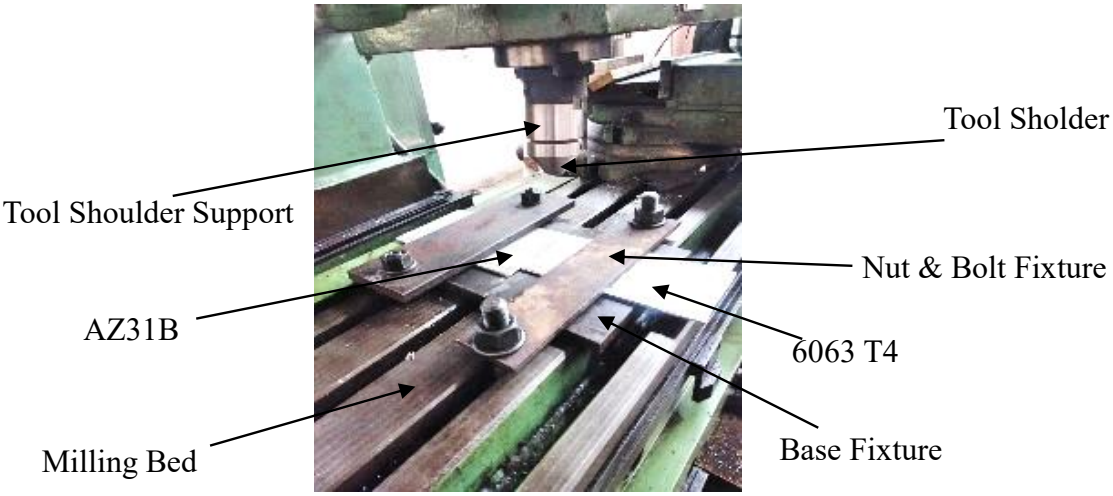

4.4: Experimental setup upon milling machine

4.2. Sample Preparation for Microstructure Analysis

Microstructural examination of the cross-sectioned tests was conducted on tests utilizing standard metallographic strategies, with the last cleaning utilizing precious stone glue of 1 and 0.25 µm molecule sizes. Chemical cleaning was at that point performed on the tests to expel any remaining fine scratches utilizing an arrangement of 2 ml HCL in 100 ml methyl liquor. The tests were carved based on the three-step strategy. The to begin with the step was to carve the tests in an arrangement of 10 ml acidic corrosive (99%), 10 ml refined water, and 4.2 g picric corrosive in 100 ml ethanol (95%) for 6 seconds to uncover the AZ31B Mg combination locales of the microstructure. The moment step was to carve the welded tests by utilizing an arrangement of 20 g NaOH in 100 ml refined water for 40 seconds to uncover the grain structure in Al 6061. The last step was to plunge them in an arrangement comprising of 4 g KMnO4 and 2 g NaOH in 100 ml refined water for 10

seconds. These three steps of the carving strategy have been connected to at the same time uncover the Al, Mg, Al3Mg2, and Al12Mg17 stages. Perception of microstructures was performed utilizing an optical magnifying instrument (ZEISS Lattice SIM 3) prepared with the image-analyzing program (aquinto Ai4).

4.2. Mechanical Testing

Every weld that was made was put through mechanical testing. Tensile testing transverse to the welding direction was used to assess the joint strength, and coupons manufactured following ASTM E8 type IV were used (dimensions are as per Figure 4.5). The specimens measured 10 mm in breadth and 100 mm in length. All tests were performed at a constant cross-head displacement rate of 1 mm/min on the FIE Make Universal Testing Machine, UTE – 40 (DSL 30). For every specimen, the highest failure load and breakdown displacement were noted. Vickers microhardness tests using the FIE Micro Vickers Hardness VM-50 was performed on the metallographic specimens under an indentation force of 100 g for 10 seconds, covering the joined nugget, agitation zone, thermomechanical affected zone (TMAZ), heat-influenced zone (HAZ), and base metal. The testing was conducted at the Kolkata, India-based Kepro Technologies NABL Testing Laboratory. Every test was run at ambient temperature.

$$Vickers\ Hardness\ (Hv): \frac{2 * F * \sin\left(\frac{136}{2}\right)}{D^2} = 1.854 * \frac{F}{D^2} \quad (4.1)$$

Where, F = Force; D = Diagonal Length

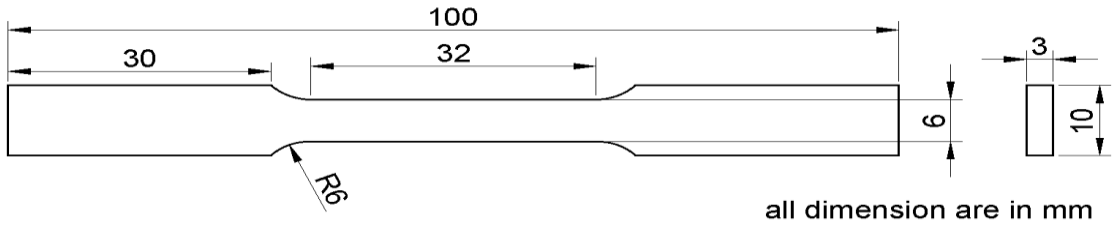

4.5: ASTM- E8- type IV dimension

4.3. Results and Discussion

4.3.1 Temperature Result

During the experiment, the workpiece's maximum temperature happens beneath the tool. The model's observed rise in temperature demonstrates that the output material's deformation from plastic and friction between the tool shoulder and the workpiece are the main causes of heat generation. The following Figures 4.6 show the temperature rise for different rotational and transit speeds.

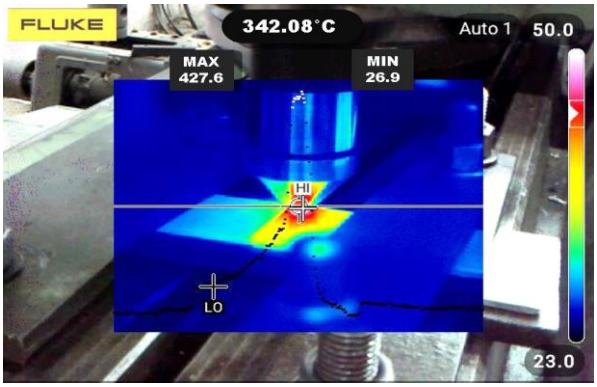

4.6(a): Temperature at 900 rpm and 25 mm/min

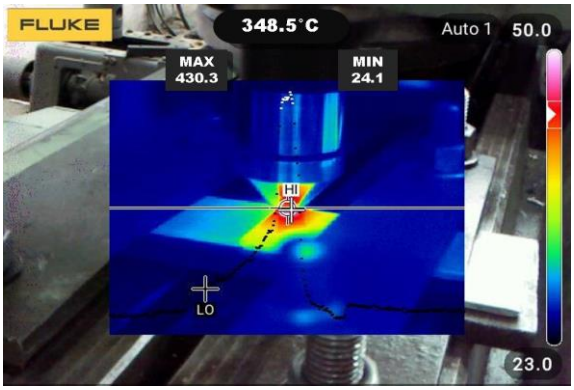

4.6(a): Temperature at 900 rpm and 40 mm/min

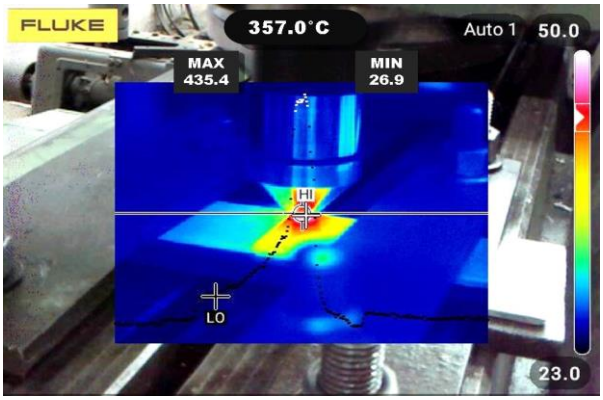

4.6(a): Temperature at 900 rpm and 63 mm/min

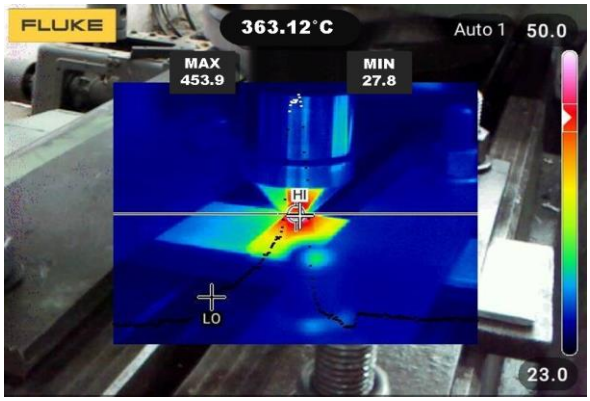

4.6(a): Temperature at 1120 rpm and 25 mm/min

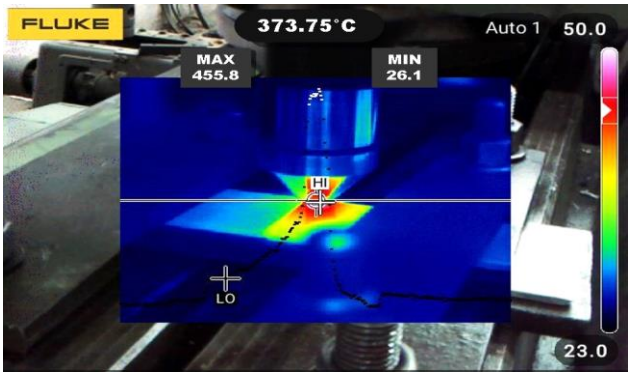

4.6(a): Temperature at 1120 rpm and 40 mm/min

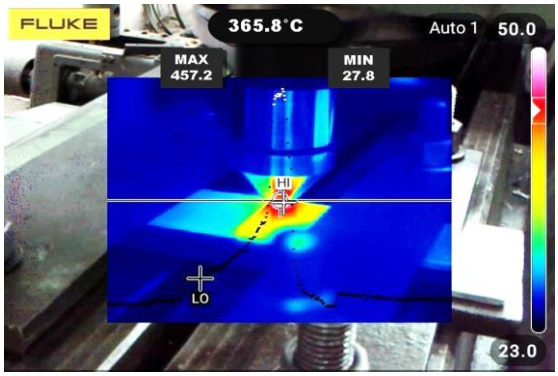

4.6(a): Temperature at 1120 rpm and 63 mm/min

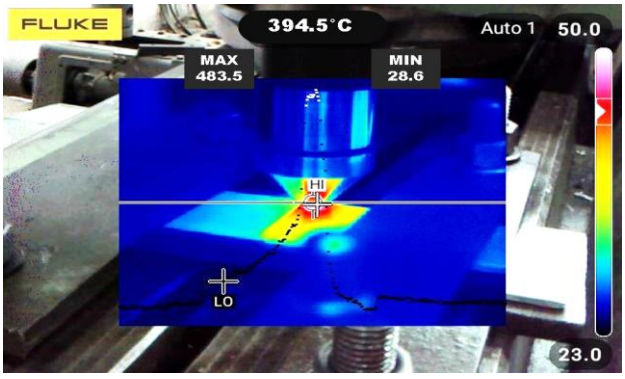

4.6(a): Temperature at 1400 rpm and 25 mm/min

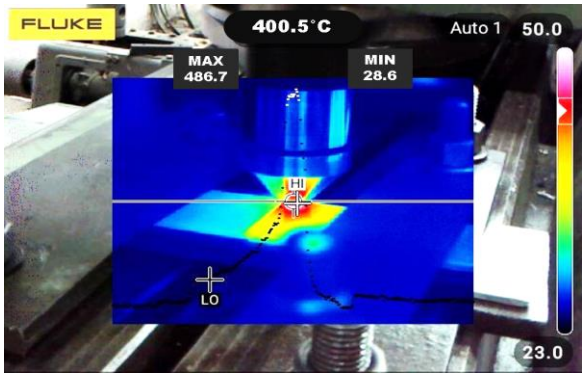

4.6(a): Temperature at 1400 rpm and 40 mm/min

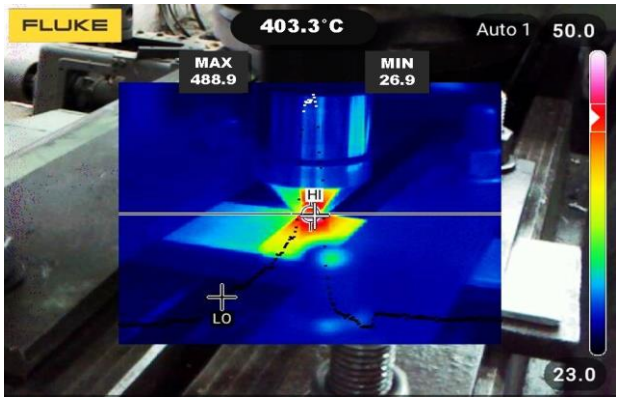

4.6(a): Temperature at 1400 rpm and 63 mm/min

4.3.2. Microstructure Analysis

The dynamic recrystallization pattern of the SZ allowed for the observation of the refined and equiaxed grains. Heat and metal deformation were the outcomes of the strained substance known as SZ. The research found that because there is more straining material in the SZ, grain size is lower and there are strain-free nucleation sites than in TMAZ, HAZ, and BM. For the above-indicated reasons, the joint formations were examined using the photomicrographs of the BM and SZ of Al 6063 t4 and Mg AZ31B at 900 rpm and 1120 rpm rotation speed and 63 mm/min travel speed.

In this investigation, the HAZ displayed some coarse and some recrystallized grains, while the SZ indicates more refined grains. There was no mechanical deformation in the HAZ, while material flow in the SZ resulted in heat cycles and mechanical deformation. Thus, heat cycles in the SZ demonstrate partial recrystallization and smaller grain due to recrystallization, with a greater effect on grain size due to dynamic recrystallization than at HAZ due to equiaxed grains. The evolution of the recrystallized grain structure in the SZ is due to the severe plastic deformation and frictional heat introduced by the rotating tool pin and its shoulder in the stir zone during welding. Since the grain size of SZ is much more refined than that of BM, grain refinement plays an essential role in material strengthening. Therefore, hardness increases as the grain size decreases. The micrographs of AZ31B and AL 6063 show that the grains are not evenly spaced and orientated. This could be a result of the different types of joints.

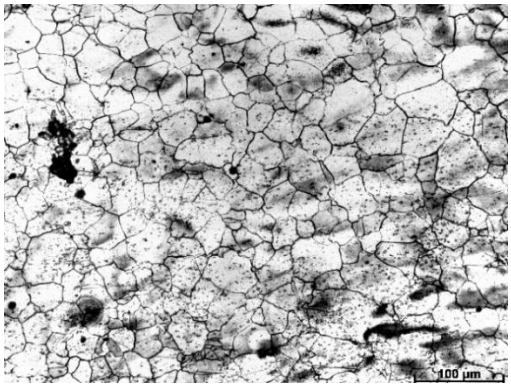

4.7(a): Microstructure of magnesium alloy BM at 900 rpm

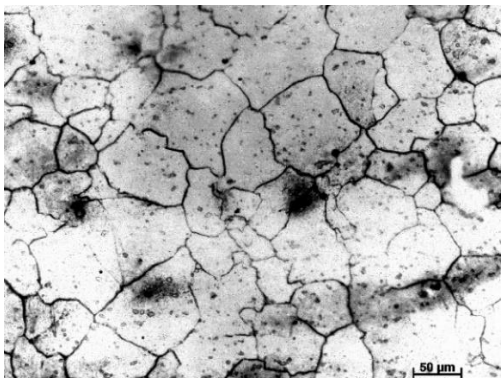

4.7(b): Microstructure of magnesium alloy BM at 1120 rpm

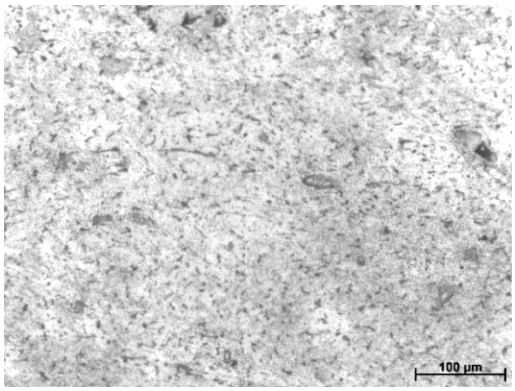

4.7(c): Microstructure of aluminum alloy BM at 900 rpm

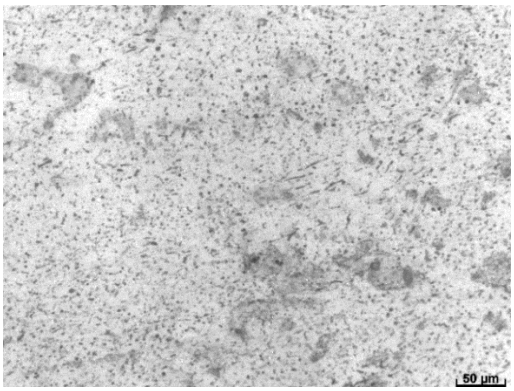

4.7(d): Microstructure of aluminum alloy BM at 1120 rpm

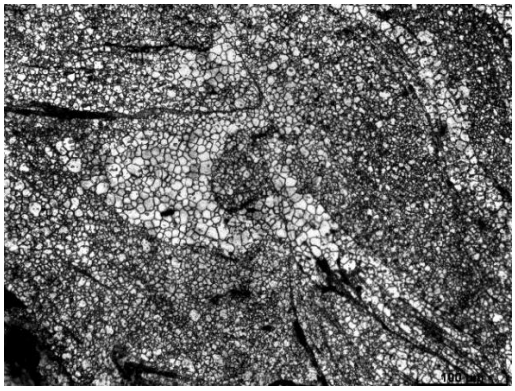

4.7(e): Microstructure of magnesium alloy HAZ at 900 rpm

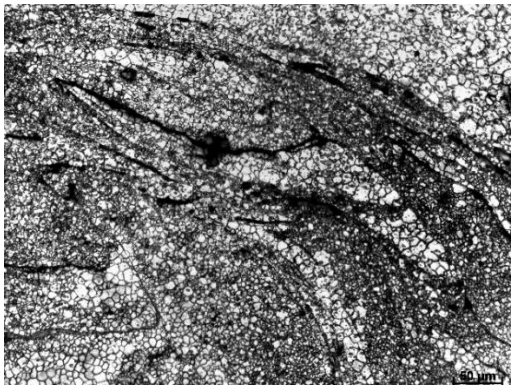

4.7(f): Microstructure of magnesium alloy HAZ at 1120 rpm

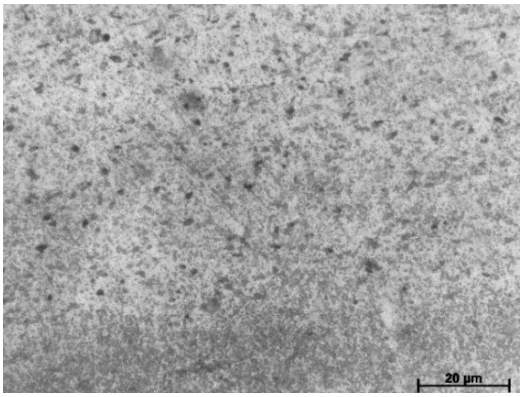

4.7(g): Microstructure of aluminum alloy HAZ at 900 rpm

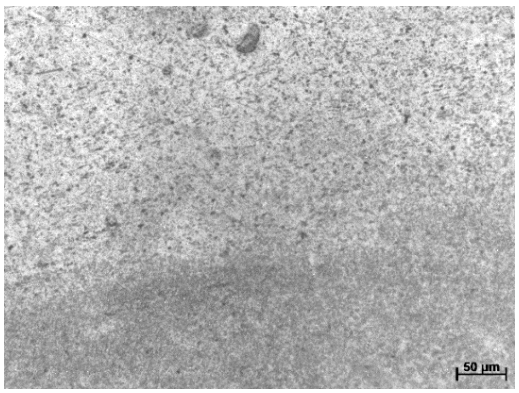

4.7(h): Microstructure of aluminum alloy HAZ at 1120 rpm

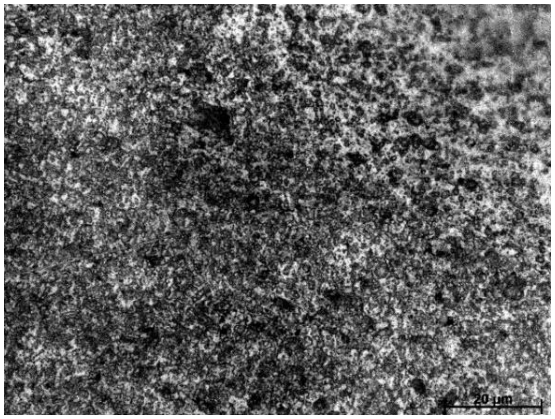

4.7(i): Microstructure of SZ at 900 rpm

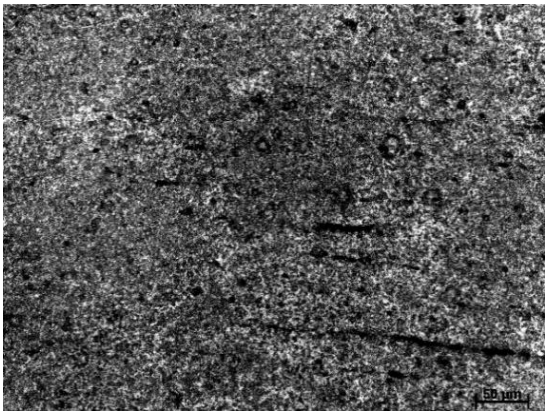

4.7(j): Microstructure of SZ at 1120 rpm

A ring-shaped onion structure was observed in the center of the weld in the SZ. Onion ring development was examined by several tests. The material in SZ moved in a ring-lipmpattern, the tool shoulder and pin were designed, and melted BM was continuously deposited between the tool shoulder and tool pin. Onion rings formed at the weld center as a result of threaded and unthreaded friction stir welding tool pins, according to prior study. Grain size and density differences lead to variations in SZ hardness, which in turn produce onion rings. The material flow on the AS was transparent and fluid, and a distinct transition zone was apparent.

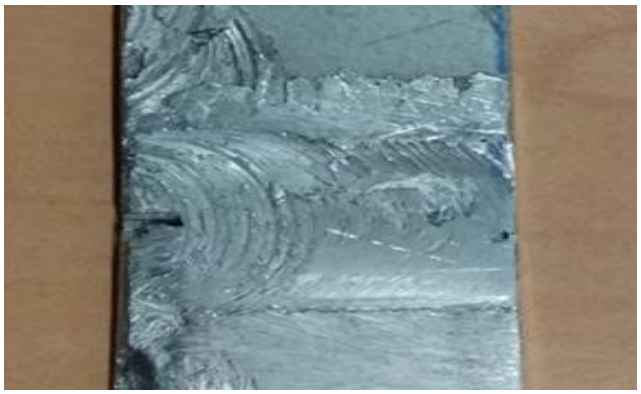

4.8: Ring-shaped onion structure

4.3.3. Microhardness Analysis

To measure the microhardness in the various friction stir welding joint zones, SZ, TMAZ, HAZ, and base material (BM) were employed. The y-axis of the graph displays microhardness in Hv, while the x-axis shows the distance from the weld centre of various butt joints. The impact of distance from the weld centre on microhardness is simulated in these graphs. The microhardness vs distance from the weld centre for the various butt joints made for three separate rotational pets (900, 1120, and 1400 rpm) and trip pets (25, 40, and 63 mm/min) is displayed in Figure 4.9.

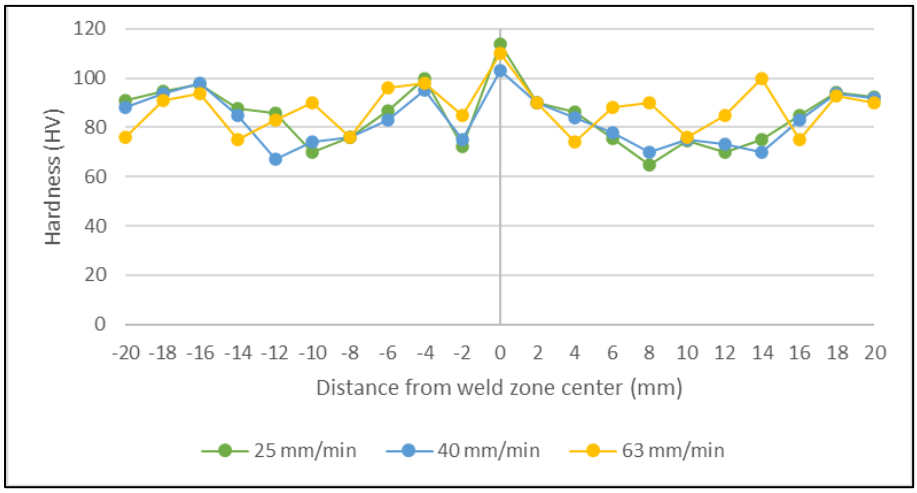

4.9(a): Microhardness of dissimilar joints attained by friction stir welding for a rotation speed of 900 rpm

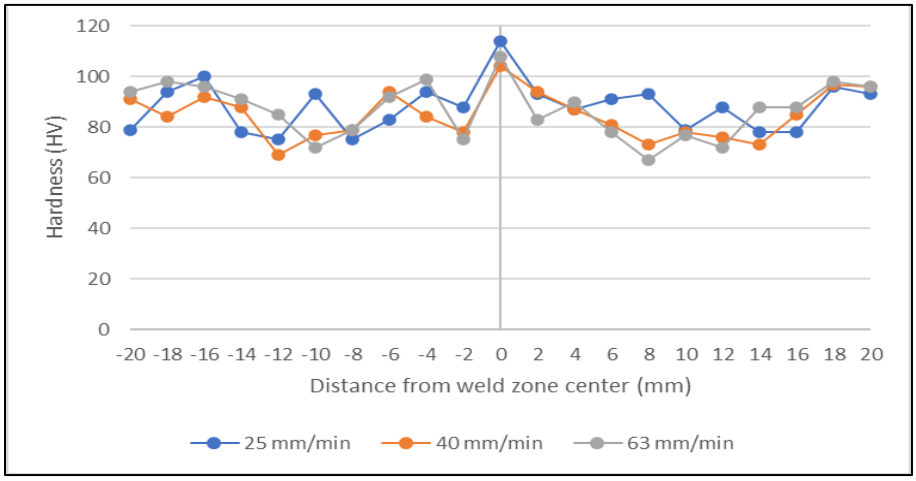

4.9(b): Microhardness of dissimilar joints attained by friction stir welding for a rotation speed of 1120 rpm

In Figure 4.9, on the x-axis, the distance from −8 to 8 shows the SZ, −8 to −12 and 8 to 12 indicates TMAZ, HAZ is indicated by −12 to −16 and 12 to 16, BM is indicated by −16 to −20 and 16 to 20. The approaching side (AS), represented by 6063 T4, is indicated by the positive sign, while the reacquiring side (RS), represented by AZ31B, is indicated by the negative sign. From an AS distance of 0 to 8 mm and an RS distance of 0 to −8 mm of the various butt joints, the tool leg directly informed the SZ of the weld. This tool leg is stirred and forged, producing heat and causing the material to mix. Figure 4.9's graphs all display an increasing trend of hardness moving from the TMAZ on both sides and towards the SZ.

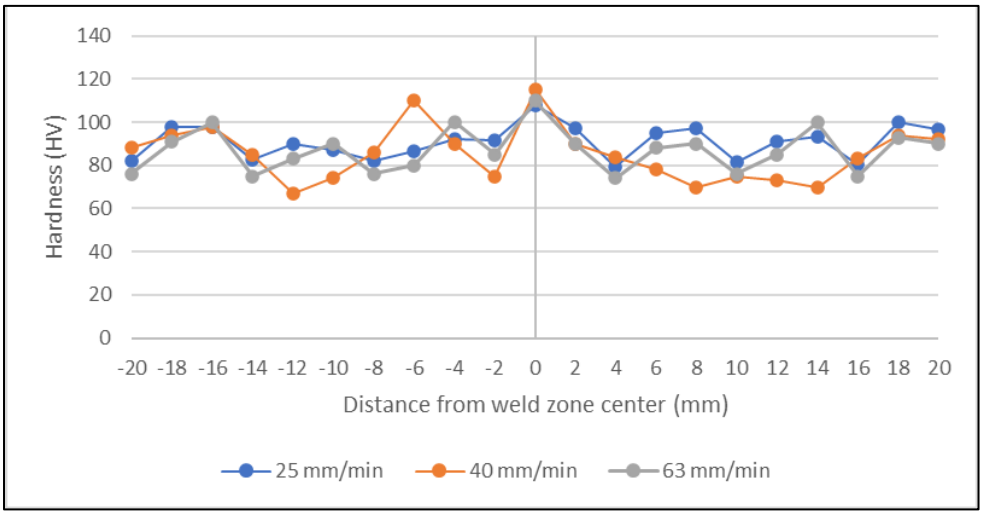

4.9(c): Microhardness of dissimilar joints attained by friction stir welding for rotation speed of 1400 rpm

The TMAZ, which spans 8 to 12 mm at the AS and −8 to −12 mm at the RS, is the conterminous zone. HAZ, measuring 12 to 16 mm on the AS and −12 to −16 mm on the RS, is the approaching zone. Because there was no mechanical shifting in these interfaces, the grain sizes of HAZ and TMAZ were smaller than those of BM, and their hardness decreased as a result. Peak temperature causes the grain of the material to soften. SZ, TMAZ, and HAZ are directly impacted by the tool shoulder due to movement, plastic distortion, stirring, mixing, and material rust. While stretching into the TMAZ region, the equiaxed grain of the HAZ region was lower concerning the foundation material. Additionally, this results in a decrease in HAZ's hardness. The next zone, BM, did not exhibit any heat-related effects.

The Al 6063 T4 and AZ31B joint was shown in Figure 4.9(a) to have a maximum hardness of 107HV at 25 mm/min, 103HV at 40 mm/min, and 106 HV at 63 mm/min in the direction of the RS. For a purported rotational speed of 900 rpm, the highest hardness values for the Al 6063 T4 and AZ31B joints were 114 HV, 108 HV, and 110 HV in the SZ. The Al 6063 T4 and AZ31B joint's RS and AS were set to a minimum hardness of 53.67 HV in TMAZ and 46.00 HV, respectively, on the AS. The advancing and reacquiring sides of BM have respective hardness values of 85.7 HV and 90.57 HV. Because AL 6063 was less hard than AZ31B, there was a change in the hardness of AL 6063 T4 and AZ31B. This was caused by the leg perimeter pushing the RS material toward the top and the AS material over. The rotating tool conveyed the workpiece material from the RS around the leg to the AS directly, and material shifting passed at the top weld.

Additionally, the joint in Figures 4.9(b) and (c) showed maximum hardness values of 95.35 HV for 25 mm/min, 104 HV for 40 mm/min, and 93 HV for 63 mm/min; additionally, the joint showed

independently maximum hardness values of 98.5 HV for 25 mm/min, 84 HV for 40 mm/min, and 93 HV at 93.62 mm/min. The maximum hardness values for the joints in the SZ were 109, 114, and 110 HV at 1120 rpm and 108, 115, and 113 HV at 1140 rpm.

4.3.4. Tensile Strength Analysis

The findings of tensile tests were used to select engineering operations' accessories. Workpieces made of aluminium and magnesium with various joints underwent a tensile test. The tensile components of the several butt joints were revealed by the collusion of the stress-strain wind. The workpiece's position of failure, yield strength, ultimate tensile strength, and extension were all related. Different joint stress-strain angles for several spinning dogs, at 900, 1120, and 1400 rpm, are shown in Figure 4.10. The y-axis on the stress-strain wind indicates the stress in megapascals (MPa), and the x-axis shows the strain in arbitrary units. The y-axis was used to determine the ultimate tensile strength and yield strength, while the x-axis was used to calculate the extension.

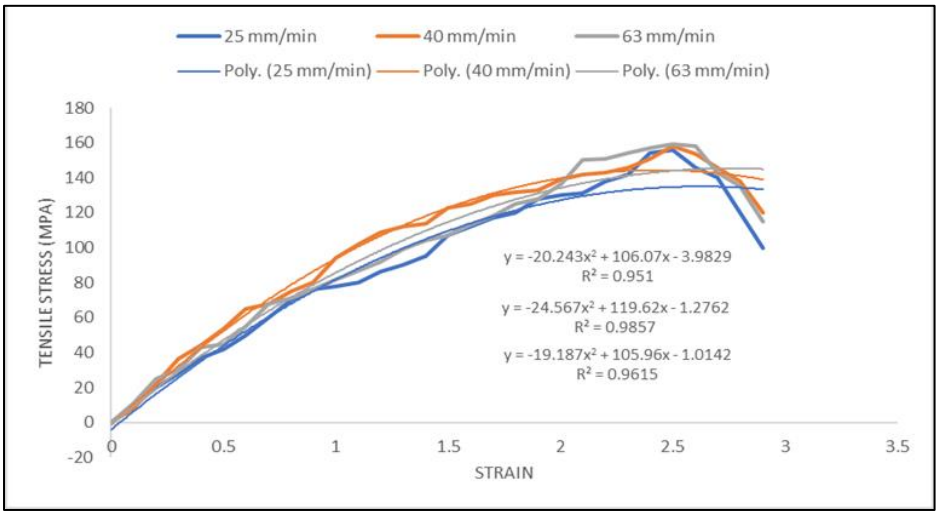

4.10(a): Stress-strain curve of the dissimilar joint of friction stir welding for rotation speed of 900 rpm

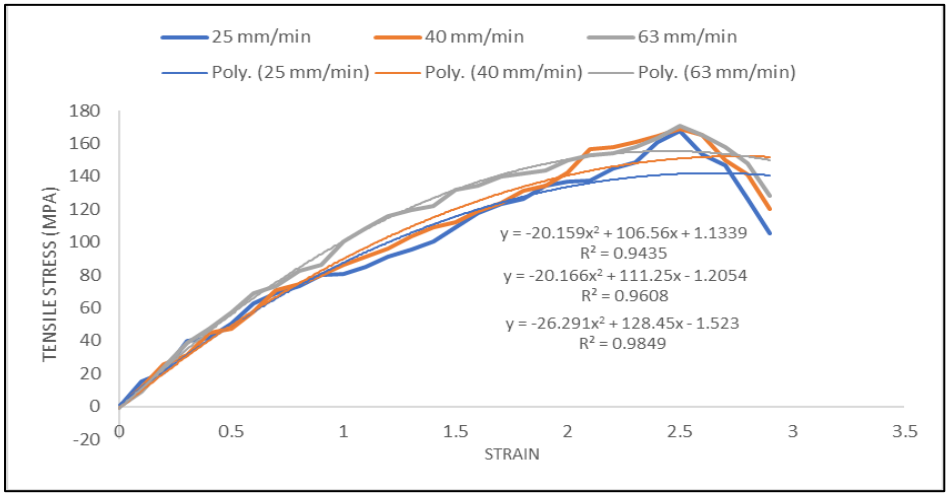

4.10(b): Stress-strain curve of the dissimilar joint of friction stir welding for rotation speed of 1120 rpm

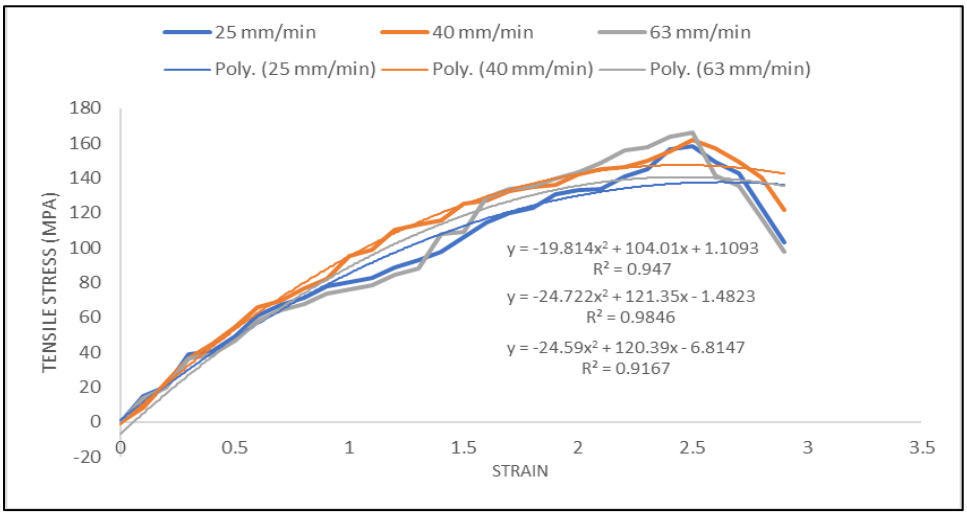

4.10(c): Stress-strain curve of the dissimilar joint of friction stir welding for rotation speed of 1400 rpm

Let us look at Figure 4.10 (a) for the Al 6063 T4 and AZ31B butt joints. The tensile strength increased from 0 to 117 MPa, 123 MPa, and 113 MPa (yield strength) with an elongation of 0 to 1.57% with travel speeds of 25, 40, and 63 mm/min. After that, the tensile strength increased slowly and remained constant up to the ultimate tensile strength, which is 155.824 MPa, 158.192 MPa, and 159.273 MPa at 3.09% elongation, respectively. Then, with a maximum elongation of 2.62%, the tensile strength dropped to 100, 120, and 115 MPa, also referred to as breaking tensile strength. Elongation and yield strength are dependent on tensile strength because tensile strength declined from both BM.

In a similar vein, the yield strengths to travel speed in Figures 4.10(b) and (c) are 123.1 MPa, 112.39 MPa, 116.1 MPa, 119.8 MPa, 125.1 MPa, and 129 MPa, respectively. Maximum elongation of 2.69% with final tensile strengths of 167.423 MPa, 168.767 MPa, 170.726 MPa, 165.077 MPa, 166.019 MPa, and 165.984 MPa. Tensile specimens Al 6063 T4 and AZ31B joint failed at TMAZ at 12, 12.9, and 11 mm for the advancing side at a rotational speed of 900 rpm due to complex extension twinning, which produced a varied texture structure and started cracks towards the advancing side. Tensile specimens AZ31 and AA6061 joint failed at TMAZ at 10, 12, and 11.5 mm retrieving side at a rotational speed of 1120 rpm. Ultimately, at TMAZ at 10, 12, and 12 mm retrieving side, the tensile specimens AZ31B and AZ91 joint failed at a rotational speed of 1400 rpm.

3.5. Summary of Experimental Result

The given table 4.1 represents the summary of experimental results including various parameters such as Rotational Speed (rpm), Travel Speed (mm/min), Temperature (°C), Maximum Micro Hardness (Hv), Average Micro Hardness (Hv), Yield Strength (MPa), and Ultimate Tensile Strength (MPa).

4.1: Summary of Experimental Result

Rotational Speed (rpm)	**Travel Speed (mm/min)**	**Temperature (°C)**	**Maximum Micro Hardness (Hv)**	**Average Micro Hardness (Hv)**	**Yield strength (MPa)**	**Ultimate Tensile Strength (MPa)**
900	25	427.6	103	93	80.211	155.824
	40	430.3	104	81	69.231	158.192
	63	435.4	108	91	67.978	159.273
1120	25	453.9	110	89	82.416	167.423
	40	455.8	114	95	71.022	168.767
	63	457.2	115	91	80.76	170.726
1400	25	483.5	108	94	80.211	165.077
	40	486.7	113	90	67.231	166.019
	63	488.9	110	92	67.978	165.984

Chapter 5

Comparative Study Between CFD Results and Experimental Results

The regions Taguchi discusses both offline and online quality control. Taguchi is a Japanese quality engineer and is known as the father of quality engineering. Cost is a key consideration when making decisions about the actions in each of these categories. Offline quality control is the process of improving quality while a product or process is being developed. "Online quality control" is the technique of keeping an eye on ongoing manufacturing procedures to verify the quality levels generated. The main distinction between a traditional experimental design and a resilient design strategy based on the Taguchi method is that the former tends to focus just on the mean of the quality characteristic, while the latter considers the minimization of the characteristic of interest's variance. Although the Taguchi approach has been found to have multiple serious shortcomings, it has proven effective in solving single-response situations. Three steps comprise the Taguchi approach, which aims to optimize a process or product design:

1. Designing a system or concept
2. Design of parameters
3. Design for tolerance

The actions to be taken for process parameter optimization are as follows:

Step 1: Choose the quality attribute that has to be improved.

Step 2: Determine the test settings and noise components.

Step 3: Create the matrix experiment and specify how the data will be analyzed.

Step 4: Carry out the matrix investigation.

Step 5: Examine the data and assume these levels of performance.

The mean was calculated to optimize the experimental welding procedure based on the desired attributes' quality. The investigation's goal function is to maximize tensile strength and hardness; so, the higher the number, the more precise the mean ratio computation will be. To obtain the higher ratio, apply the formula below:

$$Larger\ Ratio: 10 \log_{10} \frac{1}{n} \sum_{i=1}^{n} \frac{1}{Yi^2} \tag{5.1}$$

5.1. Results Analysis

5.1.1 CFD Result Analysis

5.1.1.1. Mean of Mean Ratio

The mean of the mean ratio is determined by taking the quality of the intended attributes into account. The investigation's objective function, tensile strength, is maximized to find the optimal mean of the mean ratio. Tensile strength values of the friction stir welding joints are analyzed to look into the influence of the friction stir welding process parameters. Using the CFD data, the mean of mean ratios is calculated. The average mean and primary impacts for each level are calculated and listed in Table 5.1. Better-quality qualities are indicated by a bigger mean of mean ratio, regardless of the objective function—maximization or reduction. RS2TS3 is the ideal level setting, as determined by the mean and mean of mean ratio values.

5.1: Response table for means for CFD values

Level	Rotational Speed (rpm) (RS)	Travel Speed (mm/min) (TS)
1	154.8	160.9
2	167.3	161.7
3	163.1	162.6
Delta	12.5	1.8
Rank	1	2

5.1.1.2. Analysis of Variance

The statistical determination of the relevant factor is the aim of the analysis of variance (ANOVA). It provides a clear image of the degree to which the response is influenced by the process parameter as well as the importance of the component taken into account. Tables 5.2 compute and display the ANOVA table for the mean. Figures 5.1 show the plotted main impacts for the mean. According to our research, rotating speed is a highly important component that significantly affects the tensile strength of the weld for the materials Al 6063-T4 and Mg AZ31B. The reactions are unaffected by the effect of axial force.

5.2: Analysis of variance for means of CFD tensile stress

Source	DF	Seq SS	Adj SS	Adj MS	F	P
Rotational Speed (rpm)(RS)	2	240.887	240.887	120.444	*	*
Travel Speed (mm/min) (TS)	2	4.592	4.592	2.296	*	*
Rotational Speed (rpm)* Travel Speed (mm/min)	4	0.701	0.701	0.175	*	*
Residual Error	0	*	*	*		
Total	8	246.180				

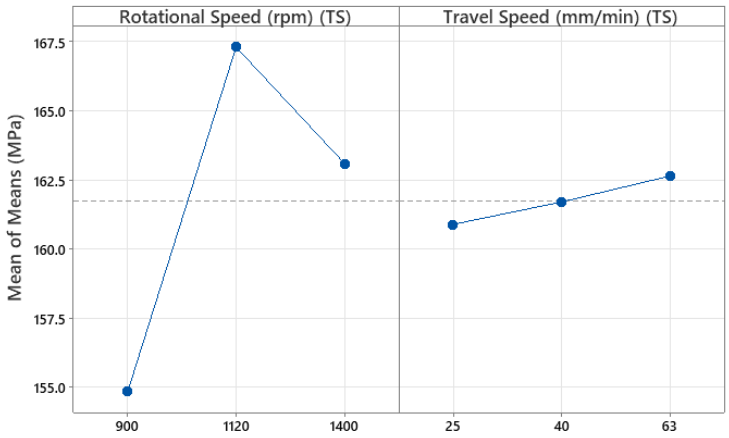

5.1: Main effects plot for means of CFD values

5.1.1.3. Estimated Tensile Strength Value

The CFD Setup and Optimisation indicate that RS2TS3 is the optimal level setting. The additive model that is utilized to evaluate the expected tensile strength is provided by the CFD analysis. The expected response value is shown below, and Table 5 provides the average values of the components at each level:

Tensile power (estimated) = RT2 + TS3 – Coef = 167.3 + 162.6 – 161.742 = 168.158 Mpa

Where RT2: rotating speed optimum mean value at two levels,

TS3: transversal speed average mean value at three tiers, and

Coef: overall mean = 161.742

5.1.2. Experimental Result Analysis

The experiment is optimized in the same way that the CFD setup is optimized. The rotational speed and travel speed are the input data, and they are compared to the material's tensile strength.

5.1.2.1. Mean of Mean Ratio

Tensile strength, hardness levels, and the effects of the friction stir welding process parameters are examined. The experimental data are used to calculate the mean. The average mean and primary impacts for each level are calculated and listed in Tables 5.3 and 5.4.

5.3: Response table for means for tensile stress value

Level	Rotational Speed (rpm) (RS)	TravelSpeed (mm/min) (TS)
1	157.8	162.8
2	169	164.3
3	165.7	165.3
Delta	11.2	2.6
Rank	1	2

5.4: Response table for means for hardness value

Level	Rotational Speed (rpm) (RS)	Travel Speed (mm/min) (TS)
1	105.0	107.0
2	113.0	110.3
3	110.3	111.0
Delta	8.0	4.0
Rank	1	2

5.1.2.2. Analysis of Variance

Tables 5.5 and 5.6 contain the generated ANOVA table for the mean. For the experimental data, the main effects for the mean are presented in Figures 5.2 and 5.3.

5.5: Analysis of variance for means of hardness

Source	DF	Seq SS	Adj SS	Adj MS	F	P
Rotational Speed (rpm)(RS)	2	99.56	99.56	49.77	*	*
Travel Speed (mm/min) (TS)	2	27.56	27.56	13.77	*	*
Rotational Speed (rpm) * Travel Speed (mm/min)	4	13.11	13.11	3.277	*	*
Residual Error	0	*	*	*		
Total	8	140.22				

5.6: Analysis of variance for means of tensile stress

Source	DF	Seq SS	Adj SS	Adj MS	F	P
Rotational Speed (rpm)(RS)	2	199.282	199.282	99.68	*	*
Travel Speed (mm/min) (TS)	2	9.928	9.928	4.969	*	*
Rotational Speed (rpm)* Travel Speed (mm/min)	4	2.384	2.384	0.591	*	*
Residual Error	0	*	*	*		
Total	8	211.594				

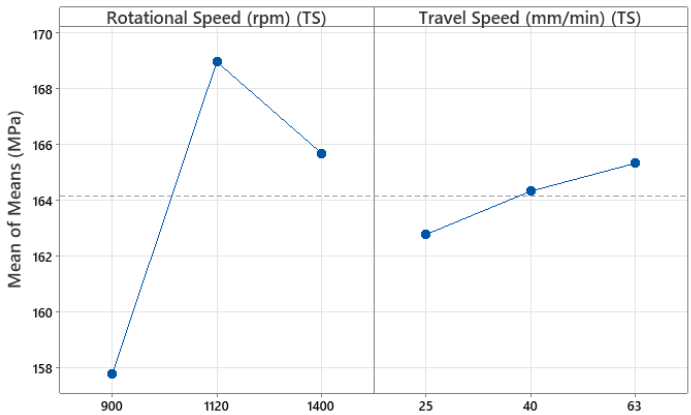

5.2: Main effects plot for means of tensile stress values

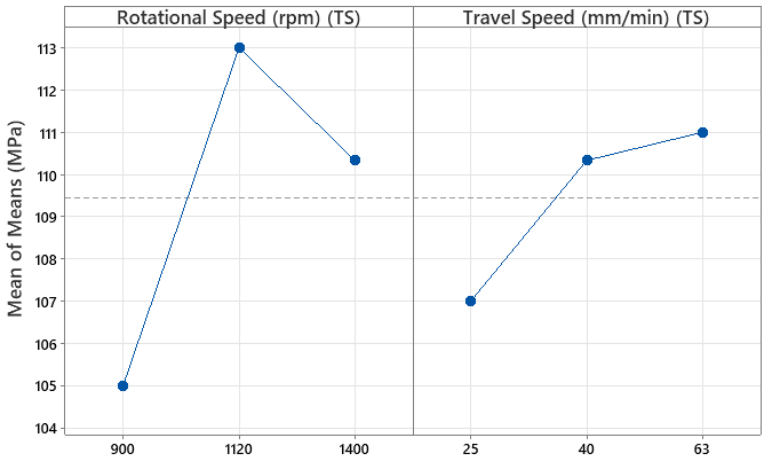

5.3: Main effects plot for means of hardness values

5.1.2.3. Estimated Tensile Strength Value

According to the experimental Setup and Optimisation, the best level setting is RS2TS3. The experimental analysis provides the additive model that is used to assess the anticipated tensile strength. The anticipated value of the response is provided below, and the average values of the components at each level are taken from Table 9:

Tensile power (estimated) = RT2 + TS3 – Coef

= 169.0 + 165.3 – 164.143

= 170.414 Mpa

Where RT2: rotating speed optimum mean value at two levels,

TS3: transversal speed average mean value at three tiers, and

Coef: overall mean = 164.143

Microhardness (predicted) = RT2 + TS3 – Coef

= 113 + 111 – 109.44

= 114.556 Hv

Where RT2: rotating speed optimum mean value at two levels,

TS3: transversal speed average mean value at three tiers, and

Coef: overall mean = 109.444

5.1.3. Verification Run

The process settings were optimized for particle and ANSYS students to conduct the confirmation trials. The transverse speed was set at 63 mm/min and the rotating speed at 1120 rpm.

5.2. Validation

The data of simulated results and experimentally measured stress and temperature using an infrared thermometer are shown in Table 5.7. The table presents a comparison between Computational Fluid Dynamics (CFD) results and experimental results across various parameters, including rotational speed, travel speed, stress, and temperature. The "Difference Percentage" columns represent the percentage difference between CFD and experimental results for stress and temperature. In general, the stress values obtained through CFD are within a reasonable range (± 1.31 to ± 1.89 MPa) compared to experimental results. However, the stress difference percentages slightly increase at higher rotational speeds (1120 and 1140 rpm) and travel speeds (40 and 63 mm/min), indicating a greater deviation between CFD and experimental results.

5.7: Comparison data of CFD and experimental result

		CFD RESULTS		**Experimental RESULTS**		**Percentage Error of CFD and Experimental**	
Rotational Speed (rpm)	Travel Speed (mm/min)	Stress (MPa)	Temperature (°C)	Stress (MPa)	Temperature (°C)	Stress (% MPa)	Temperature (% °C)
900	25	153.787	431.9	155.824	427.6	± 1.31	± 1.01
	40	154.467	434.729	158.192	430.3	± 2.35	± 1.03
	63	156.267	439.793	159.273	435.4	± 1.89	± 1.01
1120	25	166.679	458.547	167.423	453.9	± 0.44	± 1.02
	40	167.345	460.451	168.767	455.8	± 0.84	± 1.02
	63	167.865	461.88	170.726	457.2	± 1.68	± 1.02
1400	25	162.204	488.397	165.077	483.5	± 1.74	± 1.01
	40	163.282	491.625	166.019	486.7	± 1.65	± 1.01
	63	163.78	493.124	165.984	488.9	± 1.33	± 0.86

Similarly, the temperature results show a consistent trend, with CFD values being within ± 1.01 to ± 1.02°C of experimental values. However, at 1400 rpm and higher travel speeds, the temperature difference becomes more pronounced, particularly at 63 mm/min, where the percentage difference is lower for temperature compared to stress, indicating better agreement between CFD and experimental temperature results at higher speeds. In final, the stress and temperature values at the optimistic design condition are ± 1.68 and ± 1.02°C. Overall, while CFD results generally align well with experimental findings, there are slight discrepancies, especially at higher rotational and travel speeds, suggesting areas for potential refinement or calibration in the computational model.

Chapter 6

Conclusion

Based on the different AS and RS, the dissimilar joints have been friction stir welding between the Al AA6061, Mg AZ31B, and AZ91 combinations. Tensile testing, hardness testing, and CFD analysis are used to describe the different friction stir welding joints. Furthermore, a statistical analysis of the performance of dissimilar joints has been conducted. As a result, the important findings of the current investigation have led to conclusions.

- The design of the tool in friction stir welding (FSW) plays a critical role in determining the quality and efficiency of the weld joints. The geometry of the tool, including the pin and shoulder dimensions, directly influences material flow and heat generation during the welding process. To address this tool is fabricated with HSS material, prolonging tool life and maintaining weld integrity over extended periods of operation.
- This research presents a new heat transfer model that is used to model the conduction and creation of heat in friction stir welding. To verify the results of the modelling, the actual temperature has also been monitored. The heat transfer process for disunion stir welding can be modelled using this model. The temperature elaboration during friction stir welding is significantly influenced by each of the selected parameters. The investigation has led to the conclusion that a disfigurement-free disunion stir weld of 6063 T4 and AZ31B can be performed at a temperature between 430 and 490 °C.
- The microhardness of the common AL 6063 T4 and AZ31B is 104 Hv, 114 Hv, and 110 Hv at 900 rpm and 103 Hv, 114 Hv, and 110 Hv at 1120 rpm. With the trip speeds of 25 mm/min, 40 mm/min, and 63 mm/min, it is 108 Hv, 115 Hv, and 110 Hv independently for the final gyration speed of 1400 rpm, which is superior to the base accessories, which are 80 Hv for 6063T4 and 83 Hv for AZ31B. Consequently, throughout the friction stir welding process, the presence of heat encourages a joint's increasing hardness.
- Nonetheless, it has been noted that the joints' tensile strength is less than that of the foundation materials. The highest tensile strength recorded for 6063 T4 is 172 MPa, while AZ31B is 250 MPa. These values represent decreases of 2.41% and 31.2%, respectively, when compared to the relevant base material. However, at a rotational speed of 1400 rpm and a travel speed of 63 mm/min, the maximum yield strength was noted.
- The tensile strength of the joint was taken into consideration when optimizing the friction stir welding process parameters. The ideal values for the transverse and rotational speeds, respectively, are 63 mm/min and 1120 rpm. Among the tool biographies that were taken into consideration, the threaded leg tool profile was arranged to be the most fashionable.

Future Study

In contemplating the future of Friction Stir Welding for dissimilar metal materials, specifically Al6063-T4 to Mg AZ31B, several compelling avenues for further study emerge. The ongoing research in this field has already yielded valuable insights, but there remain critical areas of exploration and development

1. Material Innovation
2. Application-Specific Studies
3. Environmental Impact
4. Standardization

In conclusion, the future of friction stir welding for dissimilar metal materials holds significant promise. Ongoing and future studies will play a pivotal role in advancing the capabilities of this welding technique, making it more accessible and beneficial across various industries. Addressing these key areas of research will be instrumental in harnessing the full potential of dissimilar metal friction stir welding and meeting the evolving demands of modern manufacturing and engineering.

Publication

Two significant research papers on Friction Stir Welding of dissimilar materials have been submitted for publication, reflecting advancements in this field.

The first paper, "Characterization of Mechanical Properties of Marine Grade Dissimilar Material (AL6063 and MG AZ31B) in Friction Stir Welding," has been submitted to the prestigious journal with the help of my guide. Its manuscript number is JMEP-24-06-37502.

The second paper, titled "Microstructure Evolution and Mechanical Characterization of Dissimilar Material (AL6063-T4 and MG AZ31B) in Friction Stir Welding," was presented at the International Conference on Recent Advances in Fluid Mechanics and Nanoelectronics (ICRAFMN 2024). This conference, organised by the Manipal Institute of Technology in Jaipur, provided a platform for discussing the latest advancements and research in the field.

References

[1] AlT-S. Jun, K. Dragnevski, A.M. Korsunsky. (2010). Microstructure, residual strain, and eigenstrain analysis of dissimilar friction stir welds. *Materials and Design, 31*(2), 121-125.

[2] K. Kumar and S. V. Kailas. (2010). Positional dependence of material flow in friction stir welding: analysis of joint line remnant and its relevance to dissimilar metal welding. . *Science and Technology of Welding and Joining, 15*(4), 305-311.

[3] Murali Mohan Cheepu, V. Muthupandi, S. Loganathan. (2012). Friction welding of titanium to 304 stainless steel with electroplated nickel interlayer. *Materials Science Forum,, 710*, 620-625.

[4] Weon-kyong Kim, Byeong-choon Goo, Si-tae Won. (2010). Optimal Design of Friction Stir Welding Process to Improve Tensile Force of the Joint of A6005 Extrusion. *Materials and Manufacturing Processes, 25*, 637–643.

[5] Vijayan S, Raju R, Rao SRK. (2010). Multi-objective optimisation of friction stir welding process parameters on aluminium alloy AA 5083 using Taguchi-based grey relation analysis. *Material Manufacturing Process, 25*(11), 1206–1212.

[6] Shigematsu I, Kwon YJ, Suzuki K, Imai T, Satio N. (2003). Joining of 5083 and 6061 aluminium alloys by friction stir welding. *Journal of Material Science, 22*, 353–359.

[7] Muralimohan C H, Ashfaq M, Ashiri R, Muthupandi V and Sivaprasad K. (2016). Analysis and characterization of the role of Ni interlayer in the friction welding of titanium and 304 austenitic stainless steel Metal. *Material and Transfer, 47*, 347-359.

[8] Muralimohan C H, Haribabu S, Reddy Y H, Muthupandi V and Sivaprasad K. (2014). Evaluation of microstructures and mechanical properties of dissimilar materials by friction welding. *Material Science, 5*, 1107-1113.

[9] C.H Muralimohan, S Haribabu, Y Hariprasada Reddy, V Muthupandi, K Sivaprasad. (2015). Joining of AISI 1040 Steel to 6082-T6 Aluminium Alloy by Friction Welding. *Journal of Advances in Mechanical Engineering and Science, 1*(1), 57-64.

[10] A. Nishant A. Kamble, Second B. Omkar S. Siras. (2019). Modeling, simulation and experimental validation for friction stir welding. *International Engineering Research Journal*, 891-899.

[11] Huseyin Uzun, Claudio Dalle Donne, Alberto Argagnotto, Tommaso Ghidini, Carla Gambaro. (2005). Friction stir welding of dissimilar Al 6013-T4 To X5CrNi18-10 stainless steel. *Materials and Design, 26*, 41-46.

[12] Kush P. Mehtaa, Vishvesh J. Badheka. (2015). A Review on Dissimilar Friction Stir Welding of Copper to Aluminum: Process, Properties and Variants. *Materials and Manufacturing Processes*.

[13] A. Steuwer, M.J. Peel, P.J. Withers. (2006). Dissimilar friction stir welds in AA5083–AA6082: The effect of process parameters on residual stress. *Materials Science and Engineering, 441*, 187–196.

[14] H. H. Koo and W. A. Baeslack III. (1992). Structure, Properties, and Fracture of Linear Friction Welded AI-Fe-V-Si Alloy 8009. *Materials Characterization, 28*, 157-164.

[15] Peyre P, Sierra G, Beaume F D, Stuart D and Fras G. (2007). Generation of aluminium steel joints with laser-induced reactive wetting. *Material Science and Engineering, 444*, 327-338.

[16] Park S-K, Hong S-T, Park J-H, Park K-Y, Kwon Y-J, Son H-J. (2010). Effect of material locations on properties of friction stir welding joints of dissimilar aluminium alloys. *Science and Technology Weld Joining, 15*, 331–336.

[17] Yumeng Sun, Wenbiao Gong, Jiacheng Feng, Guipeng Lu, Rui Zhu and Yupeng Li. (2022). A Review of the Friction Stir Welding of Dissimilar Materials between Aluminum Alloys and Copper. *Metals, 12*(675), 2-26.

[18] H. Jamshidi Aval, S. Serajzadeh, A. H. Kokabi. (2011). Thermo-mechanical and microstructural issues in dissimilar friction stir welding of AA5086–AA6061. *Journal of Materials Science, 46*, 3258-3268.

[19] Zakaria Boumerzoug and Yazid Helal. (2017). Friction Stir Welding of Dissimilar Materials Aluminum AL6061-T6 to Ultra Low Carbon Steel. *Metals, 7*(42), 2-9.

[20] Won-Bae Lee, Yun-Mo Yeon, Seung-Boo Jung. (2003). The joint properties of dissimilar formed Al alloys by friction stir welding according to the fixed location of materials. *Scripta Materialia, 49*, 423-428.

[21] Won-Bae Lee, Yun-Mo Yeon, Seung-Boo Jung. (2003). The mechanical properties related to the dominant microstructure in the weld zone of dissimilar formed Al alloy joints by friction stir welding. *Journal of Material SCience, 38*, 4183 – 4191.

[22] N. Shanmuga Sundaram, N. Murugan. (2010). Tensile behaviour of dissimilar friction stir welded joints of aluminium alloys. *Materials and Design, 31*, 4184–4193.

[23] Reza Beygi, Ivan Galvão, Alireza Akhavan-Safar, Hesam Pouraliakbar, Vahid Fallah and Lucas F. M. da Silva. (2023). Effect of Alloying Elements on Intermetallic Formation during Friction Stir Welding of Dissimilar Metals: A Critical Review on Aluminum/Steel. *Metals, 13*(768), 2-25.

[24] R. Rai, A. De, H. K. D. H. Bhadeshia and T. DebRoy. (2011). Review: friction stir welding tools. *Science and Technology of Welding and Joining, 16*(4), 325-342.

[25] Li Y, Murr LE, McClure JC. (1999). Flow visualization and residual microstructures with the friction-stir welding of 2024 aluminium to 6061 aluminium. *Material Science and Engineering, 271*, 213–223.

[26] London B, Mahoney M, Bingel B, Calabrese M, Waldron D. (2001). Experimental methods for determining material flow in friction stir welds. *Proceedings of the third international symposium on friction stir welding, 271*, 213–223.

[27] R. Nandan, T. DebRoy, H.K.D.H. Bhadeshia. (2008). Recent advances in friction-stir welding – Process, weldment structure and properties. *Progress in Materials Science, 53*, 980–1023.

[28] Debtanay Das, Swarup Bag , Sukhomay Pal and Abhay Sharma. (2023). Material Defects in Friction Stir Welding through Thermo–Mechanical Simulation: Dissimilar Materials with Tool Wear Consideration. *Materials, 16*(301), 2-20.

[29] M. Koilraj, V. Sundareswaran, S. Vijayan, S.R. Koteswara Rao. (2012). Friction stirs welding of dissimilar aluminium alloys AA2219 to AA5083 – Optimization of process parameters using Taguchi technique. *Materials and Design, 42*, 1-7.

[30] C.G. Rhodes, M.W. Mahoney, W.H. Bingel, R.A. Spurling and C. Bampton. (1997). Effects of Friction Stir Welding on Microstructute of 7075 Aluminium. *ScriDta Materialia, 36*(1), 65-67.

[31] E.T. Akinlabi. (2012). Effect of Shoulder Size on Weld Properties of Dissimilar Metal Friction Stir Welds. *Journal of Materials Engineering and Performance, 21*(7), 1514-1519.

[32] A. Zens, M.F. Zaeh, R. Marstatt, F. Haider. (2019). Friction stir welding of dissimilar metal joints Rührreibschweißen von Metall-Mischverbindungen. *Materialwiss, 50*, 949-957.

[33] Xin Zhao, Fengbo Dong, Guoyou Su and Lijie Guo. (2012). Weld Quality Improvement with Hybrid FSW Technology assisted by Preheating for Copper T2/Aluminium 5A06 Dissimilar Materials. *Applied Mechanics and Materials, 121*, 1707-1711.